*J Physiol* 604.5 (2026) pp 1971–1994



The Journal of Physiology

# Role of Septin7 in mitochondrial dynamics and oxidative metabolism in C2C12 skeletal muscle cells

Andrea Telek[1,2], Ivett Gabriella Szabó[1,3], Anikó Keller-Pintér[4], Mónika Gönczi[1,2], Eliza Guti[1,2], László Szabó[1,2], Brigitta Tillmann[1,3], Zoltán Márton Kohler[4], László Juhász[5], Péter Bai[6,7,8,9], Szilárd Póliska[10], Zsuzsanna Gaál[11], László Csernoch[1,2] and János Fodor[1]

[1]*Department of Physiology, Faculty of Medicine, University of Debrecen, Debrecen, Hungary*
[2]*HUN-REN-DE Cell Physiology Research Group, University of Debrecen, Debrecen, Hungary*
[3]*Doctoral School of Molecular Medicine, University of Debrecen, Debrecen, Hungary*
[4]*Department of Biochemistry, Albert Szent-Györgyi Medical School, University of Szeged, Szeged, Hungary*
[5]*Institute of Surgical Research, Albert Szent-Györgyi Medical School, University of Szeged, Szeged, Hungary*
[6]*Department of Medical Chemistry, Faculty of Medicine, University of Debrecen, Debrecen, Hungary*
[7]*HUN-REN Cell Biology and Signaling Research Group, Debrecen, Hungary*
[8]*MTA-DE Lendület Laboratory of Cellular Metabolism, Debrecen, Hungary*
[9]*Research Center for Molecular Medicine, Faculty of Medicine, University of Debrecen, Debrecen, Hungary*
[10]*Department of Biochemistry and Molecular Biology, Faculty of Medicine, University of Debrecen, Debrecen, Hungary*
[11]*Institute of Pediatrics, University of Debrecen, Debrecen, Hungary*

Handling Editors: Karyn Hamilton & Bruno Grassi

The peer review history is available in the Supporting Information section of this article (https://doi.org/10.1113/JP288715#support-information-section).

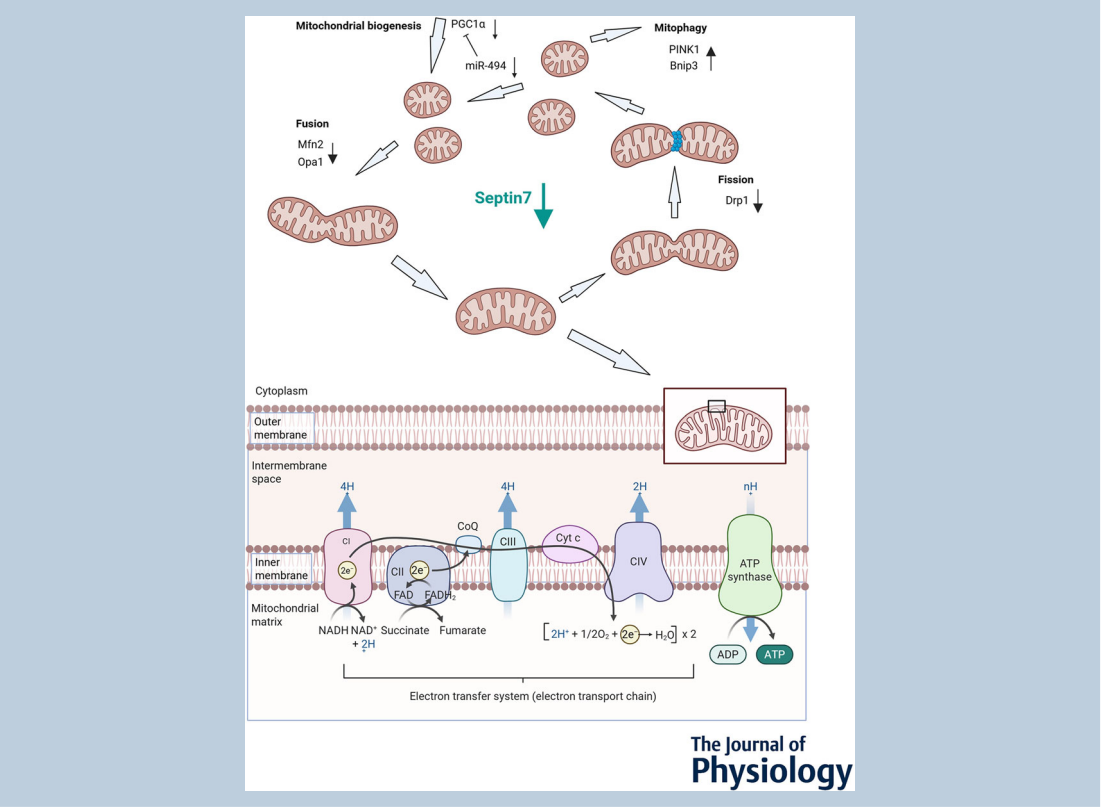


A. Telek and I. G. Szabó authors contributed equally to this work.



DOI: 10.1113/JP288715

**Abstract figure legend** Knockdown of Septin7 alters the expression of markers responsible for mitochondrial dynamics. Members of the electron transport chain are also affected by diminished Septin7 level resulting in functional changes of mitochondrial respiration.

**Abstract** Mitochondria are dynamic organelles that undergo fusion and fission. Key proteins are needed to create mitochondrial networks, as well as facilitate biogenesis, fragmentation or movement within the cell. Septins are considered as the fourth component of the cytoskeleton, providing attachment sites for proteins. Besides that, they have important roles in different cellular processes, including mitochondrial fission and fusion (remodelling). Septins form oligomeric complexes comprising various septin subgroups, which can create higher-order structures. Septin7 is the sole member of its subgroup. We aimed to examine how mitochondrial dynamics and oxidative phosphorylation (OXPHOS) are affected in Septin7 downregulated C2C12 (S7-KD) myoblasts and terminally differentiated myotubes compared to scrambled short hairpin RNA-transfected control cells. We detected altered expression of genes related to mitochondrial biogenesis (*PGC1α*), dynamics (*DRP1*, *OPA1* and *MFN2*) and autophagy (*PINK1* and *BNIP3*); furthermore, a significant decrease in differentiation-dependent mRNA expression of OXPHOS markers (*ATP synthase*, *COX1* and *SDH*). Septin7 downregulation also affected the expression of post-translational modifications of MFN2 and DRP1. Functional measurements of OXPHOS revealed decreased $O_2$ consumption (flux) and higher $O_2$ concentration in Septin7 KD cultures following selective inhibition of electron transport complexes. We observed significant alterations in basal respiration and OXPHOS pathways in Septin7 KD cultures. Our results suggest that Septin7, as a cytoskeletal protein, could be a significant regulator of mitochondrial dynamics and oxidative metabolism. Therefore, these molecules, as mitochondrial dynamics modulators, can serve as potential therapeutic targets in diseases related to changes in mitochondrial function.

(Received 10 February 2025; accepted after revision 8 January 2026; first published online 2 February 2026)
**Corresponding author** J. Fodor: Department of Physiology, Faculty of Medicine, University of Debrecen; Nagyerdei körút 98, H-4032 Debrecen, Hungary. Email: fodor.janos@med.unideb.hu

## Key points

- Knockdown of Septin7 results in altered gene and protein expression of markers controlling mitochondrial dynamics.
- Diminished level of Septin7 causes decreased gene expression of members of oxidative phosphorylation.
- Knockdown of Septin7 has an impact on microRNAs involved in the regulation of mitochondrial markers.
- Septin7 has an impact on mitochondrial respiration.

**János Fodor** earned his PhD from the University of Debrecen, Faculty of Medicine, Department of Physiology, Hungary, and completed his postdoctoral training in the Department of Physiology at the University of Debrecen. He currently serves as the research fellow at University of Debrecen, where he conducts research in the field of molecular biology.

## Introduction

Mitochondria are the powerhouse of cells, providing energy for a variety of cellular processes; in addition, mitochondria host many other functions (Casanova et al., 2023; Monzel et al., 2023). Under aerobic conditions, the electron transport chain (ETC) utilizes electron-transfer reactions to generate ATP via oxidative phosphorylation (OXPHOS) (Nolfi-Donegan et al., 2020). One of the master regulators is the peroxisome proliferator-activated receptor-gamma coactivator (PGC1$\alpha$), which co-ordinates the precise interaction between respiratory enzyme complexes required for efficient ATP production (Popov, 2020).

Energy demand of a cell/tissue partially depends on the state of differentiation (Chen et al., 2023). C2C12 is an immortalized cell line that can undergo the process of myogenesis. Upon induction of differentiation, cells transform from a mostly glycolytic myoblast to a metabolically active OXPHOS-dependent myotube (Sin et al., 2016). Adaptation to changing energy needs requires precise regulation of the mitochondria content of a cell that is achieved through regulating mitochondrial biogenesis and mitochondrial fusion and fission. Besides the aforementioned processes, this implies their degradation (mitophagy) and synthesis (biogenesis) (Pfanner et al., 2019; Wang et al., 2024). Mitochondrial biogenesis, induced by PGC1$\alpha$, could be regulated by the same network as ETC member succinate dehydrogenase (SDH) subunits, providing a link between mitochondrial function and generation of new mitochondria. On the other hand, dysfunctional mitochondria need to be removed from the cell. PTEN-induced kinase 1 (PINK1)/Parkin (Eiyama & Okamoto, 2015; Han et al., 2023; Quinn et al., 2020) and pro-apoptotic BNIP3 control mitochondrial autophagy (Ney, 2015; Zhang & Ney, 2009).

To maintain the crucial balance between fusion and fission, key proteins are needed to create mitochondrial networks, as well as facilitate fragmentation or movement within the cell (Green et al., 2022; Huang et al., 2023). Fusion and fission are mediated by large GTPase proteins from the dynamin family, such as dynamin-related protein (Drp1) (Youle & van der Bliek, 2012), which mediates fission (Banerjee et al., 2022). Mitochondria are surrounded by double membranes and for complete fusion and fission, both outer (OMM) and inner mitochondrial membranes (IMM) need to be restructured. OMM fusion is controlled by the mitofusins (Mfn1 and Mfn2), whereas IMM fusion is regulated by Opa1 (Abrisch et al., 2020). The importance of fusion and fission is supported by the fact that mitochondrial size and shape may also be directly coupled to energy production because elongated mitochondria have been shown to be correlated with more effective ATP synthesis. This phenomenon also implies to matured myofibers as glycolytic fibres showed no fusion over 30 min, whereas oxidative fibres had more interconnected mitochondria with higher fusion rates (Mishra et al., 2015).

Regulation of mitochondrial function is affected by microRNAs (miRNAs), comprsing small, non-coding RNA molecules that silence mRNA translation. Recently, certain miRNAs were found in mitochondria and hence were named mitomiRs (Geiger & Dalgaard, 2017); (Rencelj et al., 2021). Most of them are synthesized in the nucleus, but some originate from mRNA molecules transcribed from the mitochondrial genome. MitomiRs have an essential role in the regulation of mitochondrial dynamics and ATP production (Geiger & Dalgaard, 2017; Rencelj et al., 2021). Besides directly targeting relevant transcripts, miRNAs can also alter nuclear and mitochondrial gene expression (Geiger & Dalgaard, 2017). Hypoxia-associated miRNAs are miRNAs for which the expression level correlates with hypoxia and tissue damage under hypoxic conditions (Cottrill et al., 2014).

Actual energy demand requires mitochondrial transfer that occurs along the cytoskeletal system via molecular motor proteins (DeWane et al., 2021); (Illescas et al., 2021). Regulation of mitochondrial motility is incredibly important to fulfill the necessary metabolic needs upon adaptation to stressors such as reactive oxygen species (ROS), as well as to eliminate dysfunctional and aged mitochondria followed by the replenishment of healthy ones. Besides the three major components (i.e. microfilaments, intermediate filaments and microtubules), septins recently were discovered as the fourth component of the cytoskeleton providing attachment sites for proteins (Akhmetova et al., 2018; Cavini et al., 2021; Marquardt et al., 2019; Neubauer & Zieger, 2021; Wang et al., 2018). So far, 13 septin isoforms have been discovered that form hetero-oligomeric complexes and all of them contain the ubiquitous Septin7 (Gonczi et al., 2021; Gonczi et al., 2022). There is growing evidence to suggest that septins function in intracellular trafficking (Addi et al., 2018). Proteins and ion channels involved in calcium homeostasis and downstream signalling pathways require precisely orchestrated function of the cytoskeletal networks, ensuring the connection between intracellular organelles (e.g. mitochondria) within the sarcoplasma, and, finally, the link to the surface membrane (Gonczi et al., 2021; Gonczi et al., 2022; Kim et al., 2023). Consequently, it would be plausible to assume that septins participate in mitochondrial dynamics. However, so far, there is no evidence concerning the direct role of Septin7 in mitochondria dynamics. Thus, in our studies, we have focused on Septin7 to assess its importance in mitochondria function.

In our previous work, we have already shown that mitochondrial area and number were modified following the conditional knockdown of Septin7 in mice (Gonczi

et al., 2021; Gonczi et al., 2022). In Septin7-modified KD C2C12 cells, not only the filamentous structure of Septin7 was different from control cultures, but the also mitochondrial network showed alterations because long mitochondrial networks were detected within these cells. In Septin2- and Septin7 knockdown HeLa and U2OS cells, elongated mitochondria were developed as a consequence of decreased fission rather than an impaired mitochondrial fusion (Pagliuso et al., 2016). However, so far, there is no direct evidence about the role of septins in mitochondrial dynamics in myogenic cell cultures. Therefore, in the present study, we investigated the role of Septin7 (i.e. the ubiquitous member of the septin family) in mitochondrial dynamics and, consequently, in oxidative phosphorylation.

## Methods

### Cell cultures and transfection

C2C12 mouse skeletal muscle cell line was obtained from the European Collection of Cell Cultures (ECACC, Salisbury, UK) and were cultured in Dulbecco's modified Eagle's medium (DMEM; Sigma, Budapest, Hungary) supplemented with 10% foetal bovine serum (FBS), 50 U $mL^{-1}$ penicillin, and 50 μg $mL^{-1}$ streptomycin and were incubated at 37°C in a humidified incubator with 5%$CO_2$ and 95%$O_2$ in accordance with the supplier's instructions).

pGFP-V-RS-*septin7* short hairpin RNA (shRNA) vectors were stably transfected into C2C12 myoblasts using liposome-mediated transfection (Lipofectamine 2000; 11668019; Invitrogen, Waltham, MA, USA) in the presence of Opti-MEM reduced serum content medium (Thermo Fisher Scientific, Waltham, MA, USA). Cells were allowed to express the plasmid for 48 h in growth medium then were selected in DMEM containing 2 μg $mL^{-1}$ puromycin. After 5 days, puromycin-resistant transfected cells were selected. Transfection control was generated using scrambled shRNA vector and applying the same protocol; experiments were carried out on pools of scrambled transfected cells (Scr). Septin7 KD myoblasts were then differentiated into multinucleated myotubes. Cell fusion was induced at 80% confluency by exchanging the culture medium for DMEM supplemented with 4% horse serum and penicillin–streptomycin antibiotics. Downregulation of Septin7 was analysed at different developmental stages both at mRNA and protein levels. The changes resulting from Septin7 downregulation were compared with the changes observed in scrambled cells. The numbers of cell cultures and samples are indicated where appropriate because different number of cell cultures and samples were used in different experiments.

### Immunostaining and confocal imaging

Mitotracker *redCMX Ros* (M7512; Invitrogen) was applied at 0.5 μm for 30 min to stain the mitochondria. Cultured cells then were washed with ice-cold phosphate-buffered saline (0.02 M $NaH_2PO_4$ and 0.1 M NaCl), fixed in 4% paraformaldehyde for 15 min. Samples were washed three times with 100 mM glycine-phosphate-buffered saline solution for 15 min at 22°C to neutralize excess paraformaldehyde. Triton-X-100 (0.5 v/v%, 10 min, 22°C) was used for permeabilization. Non-specific biding sites were blocked with Carbo-Free Blocking Solution (SP-5040; Vector Laboratories, Burlingame, CA, USA).

Cells were then incubated overnight at 4°C with the anti-Mfn2 primary antibody (diluted 1:50 in blocking solution), corresponding to residues surrounding Val573 of human Mfn2 protein produced in rabbit, (Cell Signaling, Danvers, MA, USA), the anti-DRP1 primary antibody (diluted 1:50 in blocking solution), corresponding to residues near the amino terminus of human DRP1 protein, produced in rabbit (Cell Signaling), mouse anti-Opa1 (diluted 1:150; Invitrogen), mouse anti-MYH2 (diluted 1:500; Santa Cruz Biotechnology, Santa Cruz, CA, USA) and rabbit anti-Septin7 antibody (diluted 1:250; catalog. no. 18991; IBL Minneapolis, MN, USA). Next, Alexa 488 (Life Technologies) labelled anti-rabbit secondary antibody was applied at a dilution of 1:1000 for 1 h at room temperature. Mounting was performed with Vectashield Antifade Mounting Medium with 4′,6-diamidino-2-phenylindole (H-1200-10; Vector Laboratories). Confocal images were taken using a laser scanning confocal microscope (Zeiss LSM880 Airyscan; Zeiss, Oberkochen, Germany) with excitation wavelengthsof 405, 488 and 543 nm and using a 63× oil immersion objective.

### Transmission electron microscopic analysis

Cell suspensions from scrambled shRNA-transfected (Scr) and Septin7 knockdown (S7-KD) cultures were fixed *in situ* with fixative solution (3% glutaraldehyde in Millonig's buffer), then postfixed in 1% $OsO_4$ in water. For rapid dehydration of the specimens, graded ethanol followed by propylene-oxide intermediate was used. Samples were then embedded in Durcupan epoxy resin (Sigma-Aldrich). Ultrathin sections were cut using an Ultracut UCT ultramicrotome (Leica, Wetzlar, Germany) and stained with uranyl acetate and lead citrate. Sections were examined with a JEM1010 transmission electron microscope (JEOL, Tokyo, Japan) equipped with an camera (Olympus, Tokyo, Japan) (Gonczi et al. 2022).

### Western blot analysis

Total cell lysates were examined by western blot analysis. Samples for SDS-PAGE were homogenized

in a lysis buffer (20 mM Tris-HCl, 5 mM ethylene glycol tetraacetic acid) supplemented with Protease Inhibitor Cocktail (Sigma-Aldrich). Five-fold concentrated electrophoresis sample buffer (20 mM Tris-HCl, pH 7.4, 0.01% bromophenol blue dissolved in 10% SDS, 100 mM $\beta$-mercaptoethanol) was added to the total lysates to adjust equal protein concentration of samples and boiled for 5 min at 90°C. The samples were subjected to SDS-PAGE (10% gels were loaded with 10 μg protein per lane), transferred to BioBond nitrocellulose membranes (Cytiva, Wilmington, DE, USA) and then probed with rabbit anti-Septin7 antibody (diluted 1:250; catalog. no. 18991; IBL); mouse anti-$\alpha$-actinin (dilted 1:1000; catalog. no. sc-7453; Santa Cruz Biotechnology), rabbit anti-Drp1 antibody (diluted 1:200; catalog. no. 8570; Cell Signaling), rabbit anti-Phospho RP1Ser637 antibody (diluted 1:500, catalog. no. PA5-37534; Invitrogen), rabbit anti-Mfn2 antibody (diluted 1:1000; catalog. no. 9482; Cell Signaling), mouse anti-PINK1 antibody (diluted 1:1000; catalog. no. sc-517353; Santa Cruz Biotechnology), mouse anti-MYH2 (diluted 1:500; no. sc-71631; Santa Cruz Biotechnology) and mouse anti-Opa1 antibody (diluted 1:1000; catalog. no. MA5-16149; Invitrogen. Horseradish peroxidase-polymer-conjugated, respective anti-rabbit or anti-mouse IgG antibodies (diluted 1:1000; Bio-Rad, Budapest, Hungary) were used as secondary antibodies and the immunoreactive bands were visualized using SuperSignal West Pico or Femto Chemiluminescent Substrate (Pierce Biotechnology, Rockford, IL, USA). Immunoblots were subjected to densitometric analysis using a Gellogic 1500 system (Kodak, Rochester, NY, USA) and ImageJ (Schneider et al., 2012).

## RNA preparation, real-time PCR (RT-PCR) and quantitative RT-PCR

**RNA isolation.** Total RNA fraction was isolated with TRI reagent (MRC; cat. no. NR118; Invitrogen) from homogenized C2C12 scrambled and Septin7 KD cell cultures. The extracted RNA was resuspended in nuclease-free water and stored at −80°C. The RNA concentration and quality were analysed using a spectrophotometer at a wavelength of 260 nm (NanoDrop ND1000; Promega Biosciences, Madison, WI, USA). The isolated RNA was treated with DNase and RNase inhibitor (Ambion, Austin, TX, USA).

**Reverse transcription (RT) and quantitative PCR (qPCR).** Isolated total RNAs (1 μg) were reverse transcribed into complementary DNA (cDNA) with an Omniscript RT kit (catalog. no. 205113; Qiagen, Hilden, Germany), cDNA synthesis was pereformed using random hexamers in a reaction volume of 25 μL. For quantitative RT-PCR, TaqMan Gene Expression Assays were used with the TaqMan Gene Expression Master Mix (Applied Biosystems, Foster City, CA, USA). The amplification was performed using a Light Cycler 480 Master instrument (Roche, Basel, Switzerland) (for plates, catalog. no. 04729692001; Roche; for sealing foils, catalog. no. 04729757001; Roche). Mouse TaqMan gene expression assays were purchased from Thermo Fisher Scientific: *septin7* (Mm00550197_m1), *dnm1l* (Mm01342903_m1), *mfn2* (Mm00500120_m1), *pink1* (Mm00550827_m1), *bnip3* (Mm01275600_g1), *PGC1α* (Mm01208835_m1), *Rn18s* (Mm03928990_g1), *opa1* (Mm01349707_g1) and *mfn1* (Mm00612599_m1). The amplification program was 10 min at 95°C followed by 50 cycles of 15 s at 95°C, and 1 min at 60°C. The relative expression values for each transcript of interest were calculated by the comparative $C_t$ method and Rn18S was used for normalization.

The other set of qPCR reactions were performed with SYBR Green Mastermix (catalog. no. 04887352001; Roche), in a Light Cycler 480 Master instrument (Roche). Oligos applied for SYBR Green qPCR are listed in Table 1.

**Evaluation of qPCR data.** All qPCR reactions were conducted in triplicate. $C_p$ values were quantified with the Light Cycler 480 SW 1.5.0 software (Roche). Relative copy numbers were calculated via the $\Delta C_p$ method. The ratios of the values of the examined and normalization genes provided the relative expression levels.

**RNA-sequencing data analysis.** Isolated RNA samples were subjected to quality control by electrophoresis, followed by next-generation sequencing. Raw sequencing data (fastq) was aligned to human reference genome version GRCh38 using the HISAT2 algorithm and BAM files were generated. Downstream analysis was performed using StrandNGS software (www.strand-ngs.com). BAM files were imported and the integrated DESeq algorithm of the StrandNGS was used for quantification and normalization. A moderated *t* test was used to determine differentially expressed genes between conditions, $P < 0.05$ was considered statistically significant.

**Assessment of mitochondrial respiration.** Mitochondrial oxygen consumption was assessed ($3 \times 10^6$ cells per chamber) using High-Resolution FluoRespirometry (Oxygraph-2k; Oroboros Instruments, Innsbruck, Austria). Respiratory electron-transfer-pathway capacity (protocol I) and complex II-linked oxidative phosphorylation (OXPHOS) capacity (protocol II) were assessed in intact and digitonin-permeabilized cells.

In protocol I, complex V (or ATP synthase) was inhibited with oligomycin (2.5 μM; LEAK respiration) after stable routine respiration. The maximal capacity of the electron transport system (ETS) was reached by stepwise titration of a protonophore [carbonyl cyanide

**Table 1. Thermal profile for SYBR Green PCR comprised: initiation for 3 min at 95°C (1×); amplification: 10 s at 95°C, 30 s at 58°C, 1 s at 72°C (45×); cooling: 10 min at 40°C (1×) (Gaal et al., 2022).**

| Gene | Forward | Reverse |
|---|---|---|
| 18S | GGGAGCCTGAGAAACGGC | GGGTCGGGAGTGGGTAATTTT |
| SDH | GAACTGCACACAGACCTGC | GACTGGGTTAAGCCAATGCTC |
| COX1 | CGTTGATTATTCTCAACCAATCAC | GGTCATCTCCTAAAAGTGCACCT |
| ATP5g2 | GCTGCTTGAGAGATGGGTTC | AGTTGGTGTGGCTGGATCA |
| **miRNA** | **Stem-loop** | **Forward** |
| miR-494 | GTTGGCTCTGGTGCAGGGTCCGAGG TATTCGCACCAGAGCCAACGAGGTT | GGGTGAAACATACACGGGA |
| **Universal** | GTGCAGGGTCCGAGGT | |

*m*-chlorophenylhydrazone (CCCP); final concentration: 0.25 μM per step]. After complex I inhibition with rotenone (0.5 μM), ETS independent respiration [or residual oxygen consumption (ROX)] was determined in the presence of the complex III inhibitor antimycin A (2.5 μM). We also calculated two additional values from the obtained measurement data: one was the ATP-linked respiration (the difference between routine respiration and LEAK) and the other was the reserve capacity (the difference between ETS and routine respiration).

In protocol II, complex II-linked OXPHOS capacity was stimulated in the presence of rotenone (0.5 μM), succinate (10 mM), ADP (2.5 mM) and digitonin (40 μg $mL^{-1}$). After inhibition of ATP synthase [oligomycin (Omy); 2.5 μM], the LEAK Omy state was obtained. ROX was determined after complex III inhibition with antimycin A (2.5 μM). All measurements were performed in a Mir05 respiration medium under continuous magnetic stirring (750 rpm) at 37 °C temperature. DatLab 7.3 software (Oroboros Instruments) was used for online display, respirometry data acquisition and analysis.

**Measurement of ROS production.** Production of ROS was measured using CellRox Green Reagent for oxidative stress detection (Thermo Fisher Scientific). Three independent measurements were performed both on myoblasts (48 h after plating) and on terminally differentiated myotubes as well. ROS production was compared between scrambled and Septin7 KD cultures. Technical replicates ($n = 10$) were performed on each cell types. Cell-free loading solution served as background control. Fluorescence intensity was normalized to background. Excitation wavelength was measured at 485 nm, whereas emission was detected at 535 nm. Septin7 KD myoblasts revealed increased ROS production compared to scrambled C2C12 cells.

**Statistical analysis.** Pooled data are expressed as the mean ± SD. The differences between scrambled and Septin7 KD cells were assessed using Prism (GraphPad Software Inc., San Diego, CA, USA). We used a normality test to decide sample distribution. Pending on the result of the normality test, either an unpaired *t* test or the Mann–Whitney test was used. $P < 0.05$ was considered statistically significant. Box plot diagrams indicate the 75th and 25th percentiles (upper and lower borders of the boxes); furthermore, the minimum and maximum (whiskers), the mean value (+), the median (middle line) and the individual data points (dots) are indicated where appropriate.

## Results

### Silencing of the gene for Septin7 in C2C12 cells

Mitochondrial dynamics (i.e. fusion, fission, biogenesis and mitophagy) is co-ordinated along the cytoskeleton. Because septins are considered as the fourth component of the cytoskeleton, they play an important role in the aforementioned functions. Among the septins, Septin7 is a ubiquitous member of the group because all septin complexes contain this molecule. Therefore, we investigated the consequences of Septin7 knockdown on mitochondrial homeostasis in C2C12 cells. First, pGFP-V-RS-*septin7* shRNA was transfected into C2C12 cells to generate two different Septin7 down-regulated (Septin7 KD) C2C12 cell clones (KD1 and KD2) with reduced *septin7* expression. C2C12 myoblasts were cultured ($n = 3$ independent cultures) in DMEM supplemented with 10% FBS and 1 μg $mL^{-1}$ puromycin. To induce differentiation, FBS was replaced with 4% horse serum. Cells were harvested at 1, 3 and 5 days of differentiation, representing different stages of myotube formation. Morphological differences were visible between KD *vs.* Scr cultures. Disrupted myotube formation was detectable in KD cells, whereas, in non-transfected Scr cultures, myotube formation was completed (Fig. 1*A*). The filamentous structure of Septin7, visible in Scr myoblasts, disappeared in KD cells (Fig. 1*B*). To check the efficiency of Septin7 downregulation, qPCR

was performed. The *septin7* mRNA level was significantly lower in KD1 cultures both at the proliferation stage and at 1, 3 and 5 days after the induction of differentiation (P, D1, D3 and D5) compared to scrambled shRNA-transfected (Scr) cells. In the KD2 culture, significant *septin7* mRNA downregulation was only detectable 3 days after the induction of differentiation (Fig. 1*C*); therefore, the KD1 clone was used for most of the experiments. Septin7 downregulation was confirmed at the protein level by western blot analysis, showing 30% reduction compared to Scr cells (Fig. 1*D* and *E*).

Terminal differentiation of myotubes was confirmed by detecting the adult myosin isoform myosin heavy chain 2 (MYH2) (Fig. 2). MYH2 expression confirms that, by day 5 of differentiation, myotubes reached the terminal differentiation stage. On the other hand, MYH2-specific signals could not be detected in proliferating myoblasts (Fig. 2*C* and *D*).

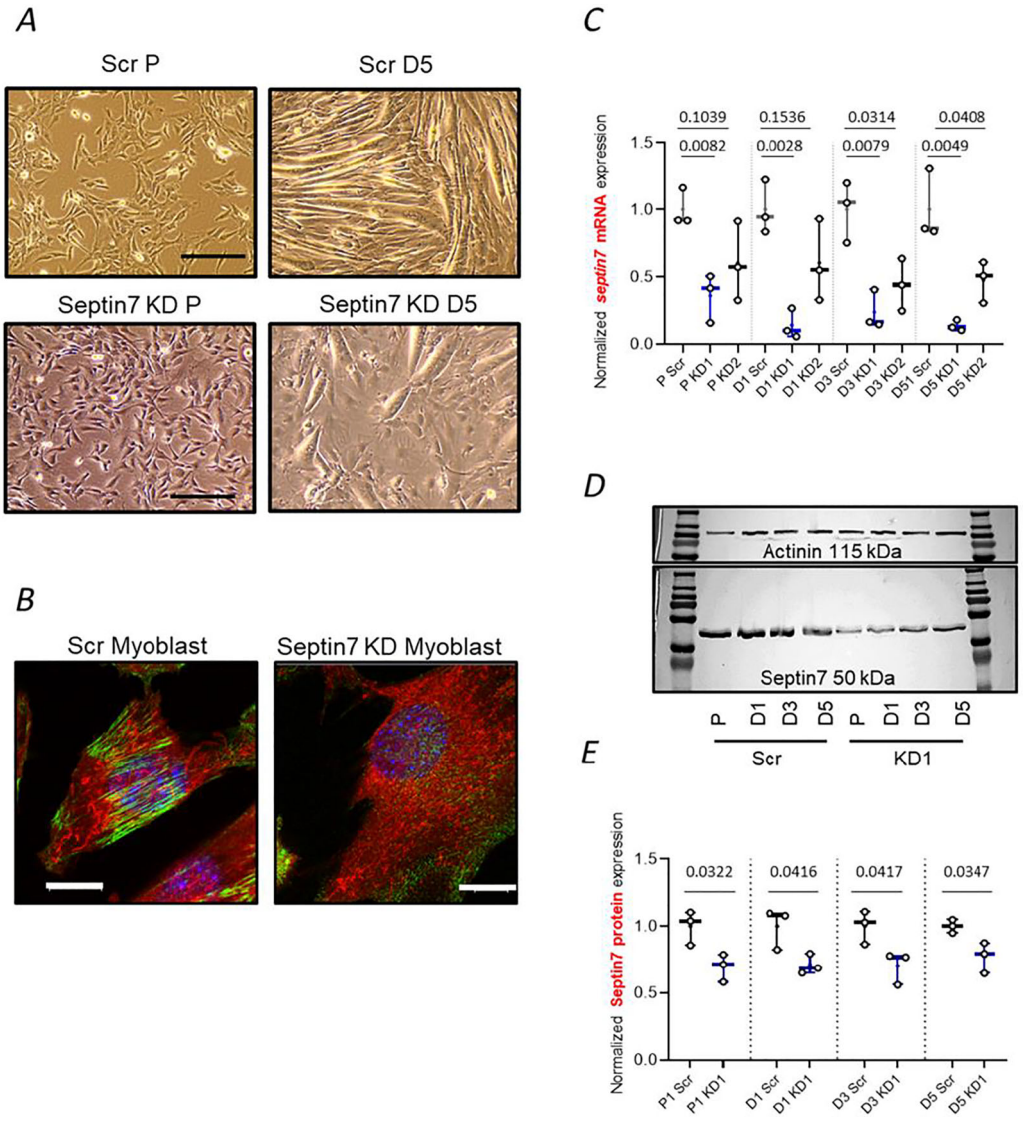


**Figure 1. Generation of Septin7 KD cells**
***A***, light microscopic analysis of scrambled and Septin7 downregulated cells in different developmental stages. P, proliferation; D5, terminally differentiated. Scale bar = 20 µm. ***B***, confocal images representing the morphology of Septin7 (Alexa488) and mitochondrial structure (Mitotracker redCMX Ros) in C2C12 myoblasts. Scale bar = 10 µm. ***C***, relative *septin7* mRNA expression (normalized to Rn18s, ribosomal) in scrambled and *septin7* KD C2C12 at different stages of differentiation (P, D1, D3 and D5) ($n$ = 3 independent cultures). ***D***, representative image of western blot showing Septin7 downregulation in KD1 cells. ***E***, relative Septin7 protein expression (normalized to $\alpha$-actinin) in scrambled and Septin7 KD1 C2C12 cells at different stages of differentiation (P, D1, D3 and D5) ($n$ = 3 independent cultures). Experiments were carried out using three independent cultures.

### Decreased Septin7 level affects mitochondrial remodelling and biogenesis

The mitochondria content of the cell needs to be increased to supply elevated energy demand of differentiating myotubes. This implies enhanced activity of mitochondrial dynamics and oxidative phosphorylation; thus, levels of regulatory markers can change during the differentiation of C2C12 cells. A diminished Septin7 level may have an impact on these processes.

Fusion, fission, iogenesis, and mitophagy markers were affected by Septin7 downregulation in both proliferating myoblasts and during myotube differentiation, as confirmeds by transcript sequencing analysis and TaqMan assays, respectively. As a result of transcriptome analysis carried out on Scr and Septin7 KD myoblasts, both the mitophagy markers (*BNIP3* and *PINK1*) and fission marker (*DNM1L*) were upregulated. On the other hand, mRNA level of ETC members (*ATP synthase*, *SDH* and *COX*) significantly decreased in KD cells (Fig. 3*A*). Transformation from proliferating myoblasts to terminally differentiated myotubes is accompanied by changes in gene expression responsible for mitochondrial dynamics

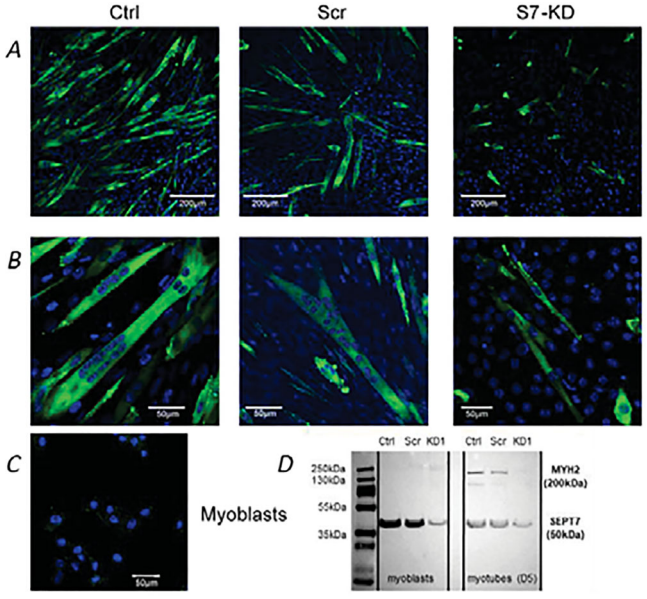


**Figure 2. Reduced expression of Septin7 results in delayed differentiation confirmed by decreased myosin heavy chain 2 level**
Confocal images of myosin heavy chain 2 (MYH2) expression in differentiating myotubes in control, scrambled and Septin7 knockdown (S7-KD) C2C12 cells, where the scale bar is 200 µm (***A***) and 50 µm (***B***), respectively. ***C***, confocal image of MYH2 expression in myoblasts (scale bar = 50 µm). ***D***, representative western blot images of MYH2 and Septin7 both at myoblast and terminally differentiated myotube stages, in control, scrambled and Septin7 KD C2C12 cells. $\alpha$-actinin was used as loading control. Splicing between the standard protein ladder and the protein bands is indicated by using dividing lines.

(Sin et al., 2016). As cell differentiation progressed, fission marker *DNM1L* mRNA was increased until day 3 of differentiation as revealed by a TaqMan assay in our experiments ($n = 4$ independent cultures). Terminally differentiated myotubes showed decreased tendency of *DNM1L* mRNA (Fig. 3*B*). Because transcript sequencing analysis could not detect altered expression of the master regulator PGC1$\alpha$, we determined its expression by a TaqMan assay. First, we studied differentiation-dependent changes in PGC1$\alpha$ mRNA level in scrambled cultures and checked whether it is being modified by Septin7 downregulation. *PGC1α* mRNA was significantly upregulated both on days 3 and 5 of differentiation compared to the myoblast stage in scrambled cultures, wheres this elevation could not be observed in Septin7 KD cells (Fig. 3*C*). To innvestigate the effect of Septin7 downregulation on mitochondria markers, scrambled and Septin7 KD myoblasts and fully differentiated myotubes were compared. *PGC1α* mRNA was significantly downregulated 5 days after the induction of differentiation (myotube stage) as a result of Septin7 downregulation (Fig. 3*D*). We observed an increasing tendency in mRNA expression of fission marker *DNM1L* in KD myoblasts stage; on the other hand, this marker became downregulated in terminally differentiated (day 5) Septin7 KD myotubes (Fig. 3*E*). Interestingly, however, mitophagy marker *PINK1* has was changed either in myoblasts or in myotubes, in contrast to the result of the sequencing analysis followed by Septin7 downregulation (Fig. 3*F*). Another pro-apoptotic marker *BNIP3* also had an increasing tendency in myoblasts, but not in myotubes (Fig. 3*G*). Mitochondrial inner membrane fusion was affected even at the myoblast stage in Septin7 KD cells as indicated by a decreasing tendency in *Opa1* mRNA. Alteration of the mitochondrial inner membrane fusion marker was more pronounced and significantly different in Septin7 KD terminally differentiated myotubes compared to scrambled cultures (Fig. 3*H* and *I*).

Besides Mfn2, Mfn1 is another GTPase dynamin-related protein located in the outer mitochondrial membrane. The mRNA level of *Mfn1* did not change significantly as a result of Septin7 downregulation in KD1 C2C12 cells, neither at the myoblast nor the myotube stage ($n = 3$ independent cultures) (Fig. 4*A*). On the other hand, expression of outer mitochondrial membrane fusion marker *Mfn2* was significantly downregulated in Septin7 KD1 cells compared to scrambled control at the same stage of differentiation ($n = 4$ independent cultures) (Fig. 4*B*). As a result of the importance of mitofusin in the regulation of mitochondrial dynamics, changes in *Mfn1* and *Mfn2* mRNA level were detected in KD2 clone as well. In KD2 clone ($n = 3$ independent cultures were used); similarly to KD1 cells, no change was observed in *Mfn1* mRNA level after Septin7 downregulation

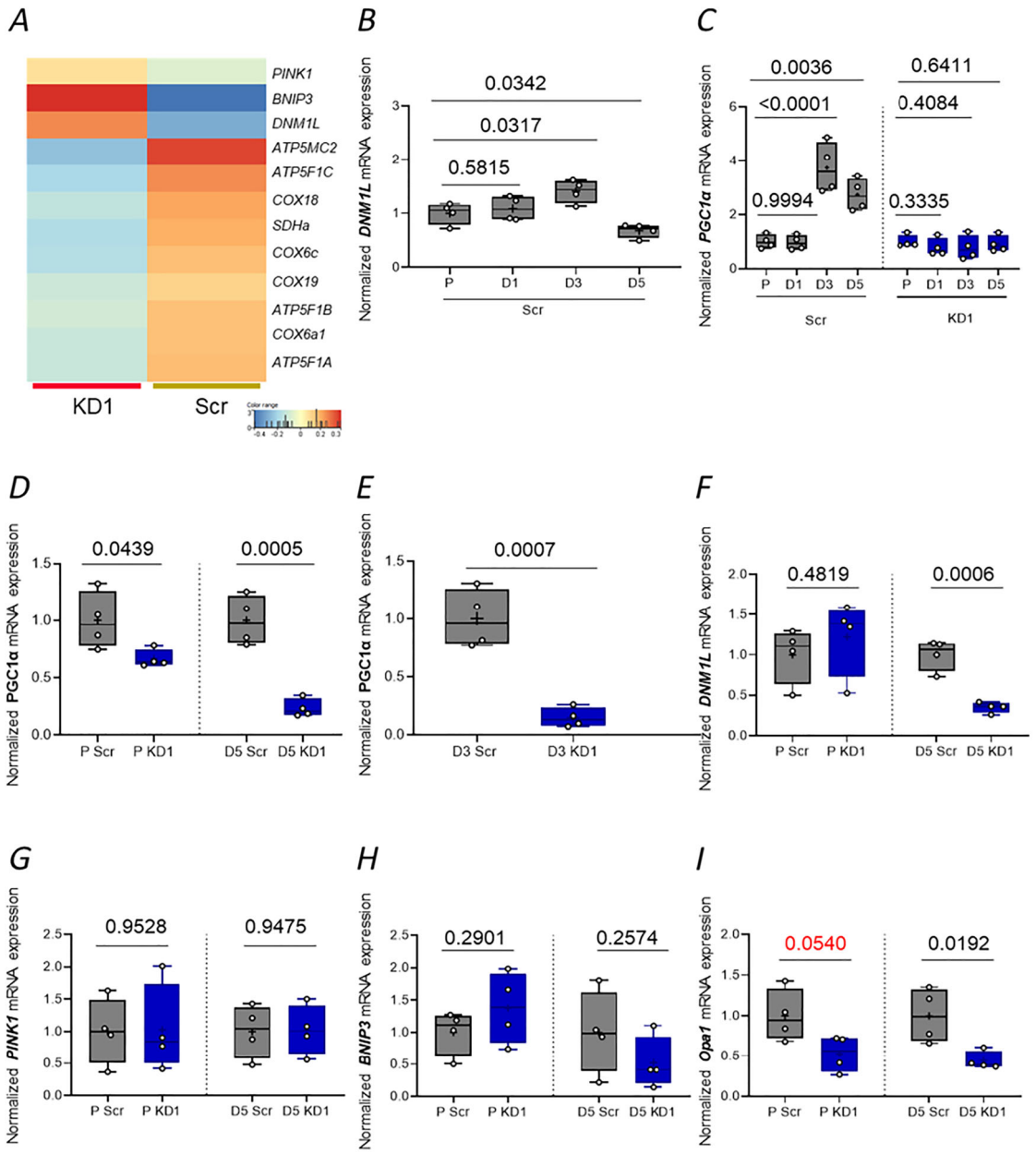


**Figure 3. Expression of mRNAs regulating mitochondrial dynamics**
*A*, heatmap showing the DESeq normalized gene expression values of '*selected genes*'. The values were calculated from three biological replicates of C2C12 myoblasts under both conditions (KD and Scr) ($n$ = 4 independent cultures). Red colour represents higher and blue colour represents lower expression level. *B*, normalized *DNM1L* mRNA expression in proliferating myoblasts (P) and differentiating myotubes at different stages of differentiation (D1, D3 and D5) in scrambled C2C12 cells. *C*, Normalized *PGC1α* mRNA expression in proliferating myoblasts (P) and differentiating myotubes at different stages of differentiation (D1, D3 and D5) in scrambled and Septin7 KD C2C12 cells. Relative (*D*) *PGC1α*, (*F*) *DNM1L*, (*G*) *PINK1*, (*H*) *BNIP3* and (*I*) *Opa1* mRNA expression (normalized to 18S rRNS) in scrambled and Septin7 KD C2C12 cells on proliferating (P) and myotube stages (D5). *E*, normalized *PGC1α* mRNA expression in differentiating scrambled and Septin7 KD C2C12 cells, 3 days after the induction of differentiation. mRNA expression was also normalized to the gene expression detected in the scrambled cultures at the same stage of development. The results in (*C*) were normalized to the proliferating stage of the cell cultures (scrambled and KD1). Experiments were carried out using four independent cultures ($n$ = 4).

downregulation (Fig. 4*A*). Interestingly, a decreased level of Septin7 resulted in a significant downregulation in *Mfn2* mRNA level in C2C12 myoblasts, but not in myotubes (Fig. 4*C*).

## Reduced Septin7 level has an impact on proteins controlling mitochondrial remodelling and biogenesis

Gene expression changes in mitochondrial quality control markers were detectable at the translational level as well. Mitochondrial fission marker *Drp1* has different post-translational modifications (Chang & Blackstone, 2010) that could be detected in scrambled transfected myotubes (indicated by a red arrow), but not in Septin7 KD cells ($n = 4$ independent cultures were used for western blot analysis) (Fig. 5*A* and *B*) (no difference was detectable at myoblast stage). On the other hand, the lower band referring to a different post-translational modification (indicated by green arrow) showed significantly increased expression in Septin7 KD myoblasts (Fig. 5*B*). Furthermore, this increasing tendency was observable even at myotube stage. Similar changes were detectable at the outer membrane fusion marker *Mfn2*, whereas the lower band referring to a different post-translational modification did not differ in scrambled and Septin7 KD cells at the myoblast or myotube stage. Two different post-translational modifications could be observed at the inner membrane fusion marker *Opa1* as well (Fig. 5*A* and *B*). The intensity of the lower band did not reveal a significant difference either at the myoblast stage (P) between scrambled and KD cultures or at the myotube stage (D5) between the two cell types, respectively. In terms of all the markers examined, the lower band had stronger expression at the terminally differentiated stage *vs*. myoblasts in both cell types, whereaqs knockdown of Septin7 resulted in a weaker band by day5 for *Mfn2* and *Opa1* expression. We observed that Septin7 downregulation altered the morphology of both C2C12 cells and mitochondria as well. Co-localization between mitochondria and mitochondrial markers could be detected by immunocytochemistry. We observed an altered and disrupted mitochondrial network; furthermore, multinucleated myoblasts were detected due to impairment of cytokinesis in Septin7-KD cells (Fig. 5*C*).

In the next step, we aimed to verify whether the post-translational modifications correspond to the phosphorylated forms of DRP1 (pDRP1Ser616 and pDRP1Ser637) (Fig. 6*A* and *B*). Expression of pDRP1Ser637 could be detected in both myoblasts and myotubes as well. Septin7 downregulation resulted in significant downregulation of pDRP1Ser637 in both myoblasts and myotubes compared to scrambled control ($n = 3$ independent cultures were used for the analysis). On the other hand, expression of pDRP1Ser616 could not be detected. Mitophagy marker *PINK1* showed a declining tendency in Septin7 downregulated myotubes compared to scrambled cultures ($n = 4$ independent cultures were used for the analysis except for the proliferating KD1 cells, where we used three independent cultures) (Fig. 6*C* and *D*).

To investigate whether there is any link between Septin7 downregulation and changes in mitochondrial markers, in other words, whether alterations of cytoskeleton affect mitochondria, colocalization of Septin7 and Opa1 was assessed by immunolabeling conducted in both proliferating myoblasts in scrambled ($n = 11$ cells) (Fig. 7*A*) and Septin7-KD ($n = 14$ cells) (Fig. 7*B*) cultures. However, weak colocalization and overlapping of Opa1 and Septin7 were determined by calculating Pearson and Manders' coefficients, respectively; these parameters were significantly reduced in Septin7-KD myoblasts compared to control and scrambled cultures (Pearson: Scr *vs*. KD: $P = 0.029$; Manders: Scr *vs*. KD: $P = 0.00022$) (Fig. 7*C*).

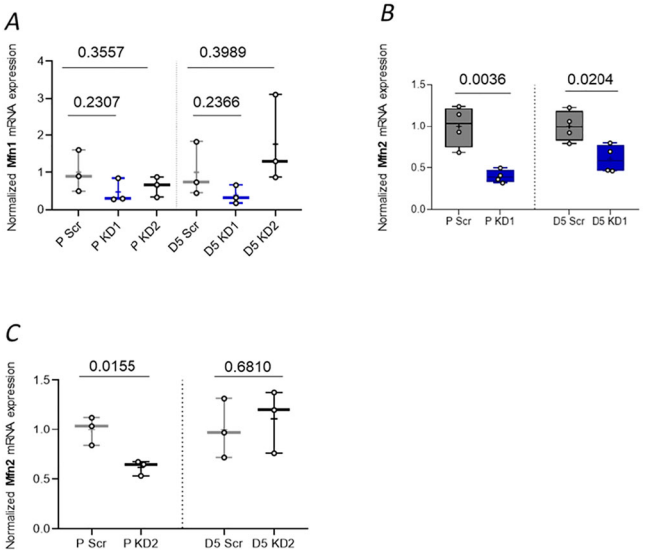


**Figure 4. Expression of mRNA affecting mitochondrial dynamics is altered as a result of Septin7 downregulation**
*A*, normalized *Mfn1* mRNA expression in proliferating myoblasts (P) and differentiating myotubes (D5) in scrambled and Septin7 KD1 and KD2 C2C12 cells ($n = 3$ independent cultures). *B*, normalized *Mfn2* mRNA expression in proliferating myoblasts (P) and differentiating myotubes (D5) in scrambled and Septin7 KD1 C2C12 cells. Experiments were carried out using four independent cultures ($n = 4$). *C*, normalized *Mfn2* mRNA expression in proliferating myoblasts (P) and differentiating myotubes (D5) in scrambled and Septin7 KD2 C2C12 cells ($n = 4$ independent cultures). mRNA expression was also normalized to the gene expression detected in the scrambled cultures at the same stage of development.

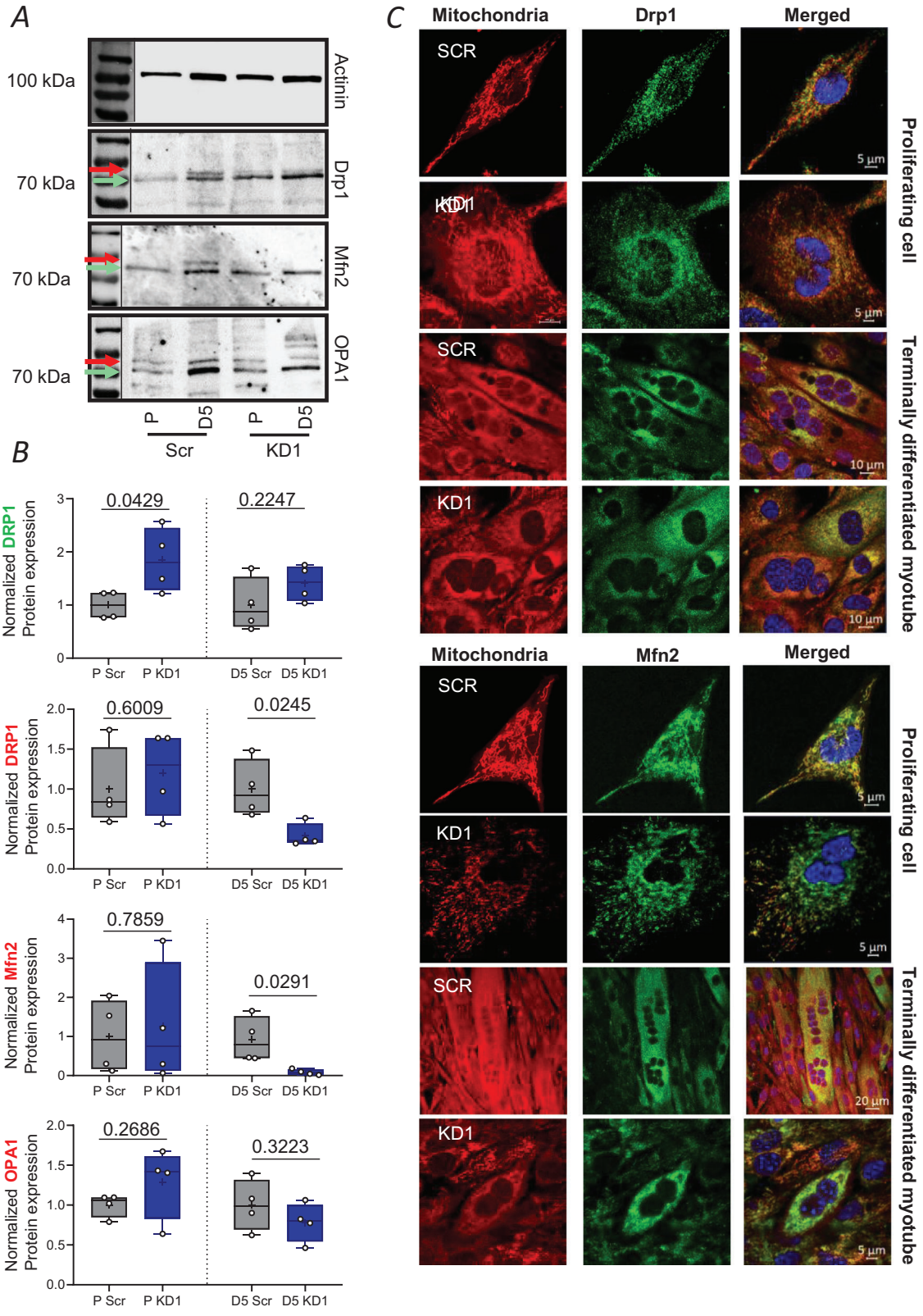


**Figure 5. Decreased Septin7 alters the structure of mitochondria and the expression of markers responsible for mitochondrial dynamics**
*A*, representative western blot images of mitochondrial dynamics marker *Drp1*, *Mfn2* and *Opa1* both at the myoblast and terminally differentiated myotube stage in scrambled and Septin7 KD C2C12 cells. $\alpha$-actinin was used as

loading control. Splicing between the standard protein ladder and the protein bands is indicated by using dividing lines. *B*, quantitative analysis of *Drp1*, *Mfn2* and *Opa1* expression in scrambled and Septin7 KD C2C12 cells at the myoblast and terminally differentiated myotube stages ($n$ = 4 cultures were used for the analysis). *C*, confocal images of mitochondria (redCMX Ros) *Drp1* and *Mfn2* (Alexa488) expression in proliferating myoblasts (P) and in terminally differentiated myotubes in scrambled and Septin7 knockdown C2C12 cells.

## Septin7 downregulation results in decreased expression of the key members of oxidative phosphorylation

It is plausible to assume that septins affect mitochondrial functions besides dynamics. Indeed, mRNA levels of respiratory chain members are significantly diminished in KD cells. SDH (also known as ETC complex II) mRNA was significantly lower in KD cells in myoblasts and at day 1 after the induction of differentiation. On the other hand, *SDH* gene expression level did not change significantly at latter time points. Changes of expression pattern were the same for complex IV (cytochrome *c* oxidase) and V (ATP synthase) as mentioned in the case of SDH (Fig. 8*A*–*C*) ($n$ = 4 independent cultures). Regulation of mitochondrial function is also affected by miRNAs that interfere with mRNA translation. Besides PGC1$\alpha$, miRNAs also regulate the function of the respiratory chain complex. *miR-494* inhibits PGC1$\alpha$ and complex V. *MiR-494* expression had an increasing tendency in KD cells at day 3 after the induction of differentiation compared to scrambled cells ($n$ = 4 independent cultures). This can explain the lack of increase in *PGC1α* mRNA in KD cells. Interestingly, the tendency reversed by day 5

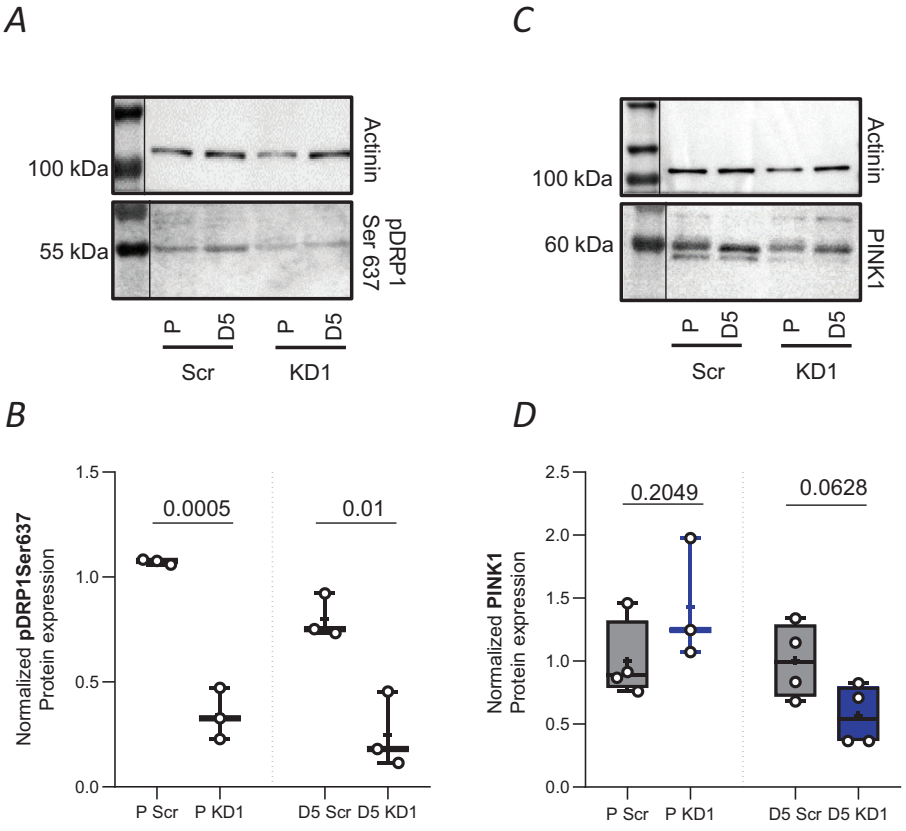


**Figure 6. Expression of proteins affecting mitochondrial dynamics is altered as a result of Septin7 down-regulation**
*A*, representative western blot images of mitochondrial dynamics marker pDRP1Ser637 in myoblasts and terminally differentiated myotubes in scrambled and Septin7 KD C2C12 cells. $\alpha$-actinin was used as loading control. Splicing between the standard protein ladder and the protein bands is indicated by using dividing lines. *B*, quantitative analysis of pDRP1Ser637 protein expression in scrambled and Septin7 KD C2C12 cells at myoblast and terminally differentiated myotube stages ($n$ = 3 independent cultures). *C*, representative western blot images of PINK1 in myoblasts and terminally differentiated myotubes in scrambled and Septin7 KD C2C12 cells. $\alpha$-actinin was used as loading control. *D*, Quantitative analysis of PINK1 protein expression in scrambled and Septin7 KD C2C12 cells at myoblast and terminally differentiated myotube stages ($n$ = 4 independent cultures were used for the analysis except for the proliferating KD1 cells, where we used three independent cultures).

because *miR-494* expression was lower in Septin7 KD cells *vs*. Scr cells. However, this difference was not significant. (Fig. 8*D*). An increasing tendency could be detected in the production of ROS in Septin7 KD cells compared to scrambled control in the same day of differentiation ($n = 3$ independent cultures) (Fig. 8*E*).

### Septin7 deficiency decreases oxidative metabolism in both myoblasts and myotubes

We investigated mitochondrial function in Septin7 silenced myoblasts and myotubes both on KD1 (Fig. 9) and KD2 clones (Fig. 10), respectively. Two different protocols were used on a high-resolution respirometer. First, myoblasts ($n = 11$–13, others: $n = 6$–8 were in KD1 myoblasts, whereas, in the case of KD2 myoblasts Routine and ROX: $n = 11$–13, others: $n = 6$–7, respectively) were examined using protocol I, which allowed us to determine routine respiration, LEAK, ETS, ROX and the two calculated values, ATP-linked respiration and reserve capacity (Figs 9*A* and *C* and 10*A* and *C*). Silencing Septin7 reduced the routine respiration, LEAK and ROX values of the myoblasts (Figs 9*C* and 10*C*). Subsequently, protocol II was also applied on myoblasts, allowing us to measure routine respiration, along with complex I-dependent respiration OXPHOS capacity and the LEAK Omy state (Figs 9*B* and *C* and 10*B* and *C*). As a result of Septin7 deficiency, complex I-linked $O_2$ consumption, OXPHOS and LEAK Omy state were also reduced in myoblasts (Figs 9*C* and 10*C*). Furthermore, we also investigated oxidative phosphorylation in permeabilized and non-permeabilized myotubes using the same respirometric protocols applied in myoblasts (Figs 9*D* and *E* and 10*D* and *E*). We found that silencing of Septin7 resulted in reduced routine respiration, OXPHOS and LEAK Omy state in myotubes (Figs 9*D*–*F* and 10*D*–*F*) (Routine and ROX: $n = 12$–16, others: $n = 6$–8 were in KD1 myotubes, whereas, in the case of KD2 myotubes Routine and ROX: $n = 16$–17, others: $n = 8$–9, respectively).

Changes in the mitochondrial network were not reflected in the changes of the inner mitochondrial structure (Fig. 11*A* and *B*). Using high magnification of transmission electron microscopy, mitochondrial units with various shapes were observed. However, a significant difference in the inner mitochondrial structure could not be described between Scr and Septin7-KD samples ($n = 2$ independent cultures; images were taken from seven different slides in the case of scrambled cells and 14 different slides in the case of KD cells, respectively).

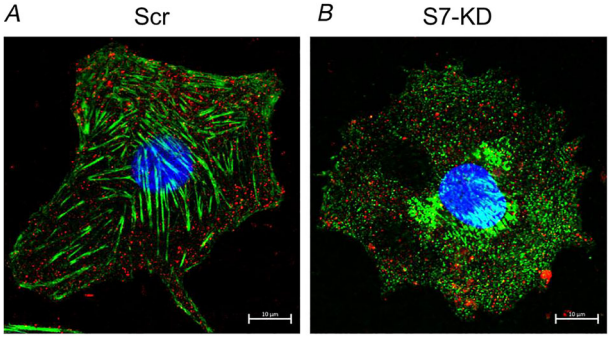


C

| | Scr | S7-KD |
|---|---|---|
| Pearson (Mean ± SD) | 0.071±0.020 (n=11) | 0.054±0.017* (n=14) *p<0.05 (vs. Scr) |
| Manders (Opa1 overlapping Septin7) (Mean ± SD) | 0.262±0.034 | 0.186±0.067* *p<0.005 (vs. Scr) |

**Figure 7. Septin7 knockdown results in altered colocalization between Septin7 and Opa1**
Intracellular expression and localization of Septin7 (green) and Opa1 (red) proteins were determined in scrambled shRNA-transfected (Scr) ($n = 11$ cells) (*A*) and Septin7-KD (S7-KD) myoblasts ($n = 14$ cells) (*B*) using high-resolution confocal microscopy following immunolabeling. Colocalization of the fluorescence signals were determined by two methods, where Pearson correlation quantifies the degree of colocalization between two different fluorescence signals by measuring the linear relationship between their pixel intensities, whereas Manders' coefficient is a value specifically measuring the fraction of signal from one fluorophore that overlaps with the signal from another fluorophore. Both correlation analyses revealed significant difference between Septin7-modified cultures compared to Scr cells (Pearson: Scr *vs*. KD: $P = 0.029$; Manders: Scr *vs*. KD: $P = 0.00022$). Scale bars = 10 μm (*C*).

## Discussion

In the present study, we aimed to investigate the role of Septin7 in mitochondrial dynamics and oxidative metabolism. We found that decreased Septin7 level has an impact both on the expression of markers of mitochondrial dynamics and mitochondrial functions as well. Multifaceted mitochondria have diverse function in the majority of the cells. Besides energy production via oxidative phosphorylation, they play an important role in the regulation of cellular $Ca^{2+}$ homeostasis, heat production, cell proliferation and apoptosis. All of these require precise regulation of mitochondria number and size by processes called biogenesis, dynamics and mitophagy. Here, we investigated the consequences of Septin7 downregulation on mitochondrial dynamics and its functional consequences on cellular respiration.

Adaptation to changing energy needs is inevitable for the cells, which implies mitochondrial transfer within the cell to the exact location where energy demand is the highest (Chen et al., 2023; Green et al., 2022; Wang et al., 2024). Accumulating evidence suggests the critical role of the cytoskeletal system in mitochondrial

motility as well as in dynamics (Illescas et al., 2021). Actin filaments are required for the proper formation of mitochondria-endoplasmic reticulum contacts (MERCs), known as ERMES (ER-mitochondria encounter structure) in yeast (Kornmann & Walter, 2010). In neurons, mitochondria are coupled to microtubule motor proteins (kinesins and dyneins), forming a motor complex together with the OMM GTPase Miro and the adaptor protein Milton/TRAK that mediates long-range mitochondrial transport (Hirokawa & Takemura, 2005; Kruppa & Buss, 2021; Schwarz, 2013; van Spronsen et al., 2013). Besides well known parts of the cytoskeleton (microtubules, microfilaments and intermedier filaments), septins are considered as the fourth component of this network. Based on our previous results (Gonczi et al., 2021; Gonczi et al., 2022; Szabo et al., 2023) and on studies from different research groups (Addi et al., 2018; Marquardt et al., 2019; Wang et al., 2018), accumulating evidence suggests that this newly discovered cytoskeletal component has an important function in intracellular trafficking.

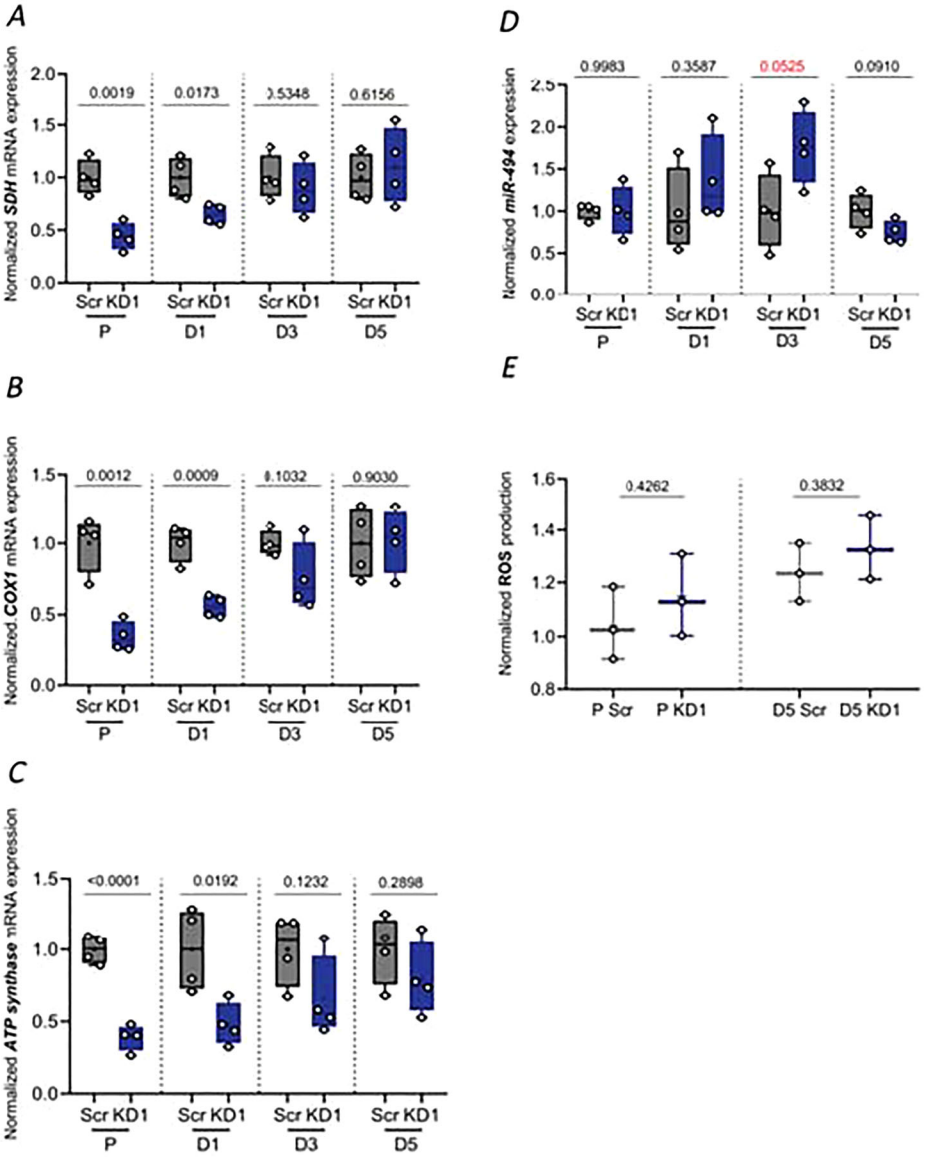


**Figure 8. Decreased *septin7* expression affects mitochondrial metabolic activity**
Relative (*A*) *SDH*, (*B*) *COX1* and (*C*) *ATP synthase* mRNA expression (normalized to Rn18S) ($n$ = 4 independent cultures); relative (*D*) *miR-494* expression in scrambled and Septin7 KD C2C12 cells in proliferating myoblasts (P) and myotubes at different stages of differentiation (D1, D3 and D5) ($n$ = 4 independent cultures). *E*, production of ROS in scrambled and Septin7 KD C2C12 cells in proliferating myoblasts (P) and differentiated myotubes (D5) (normalized to cell free dye) ($n$ = 3 independent cultures).

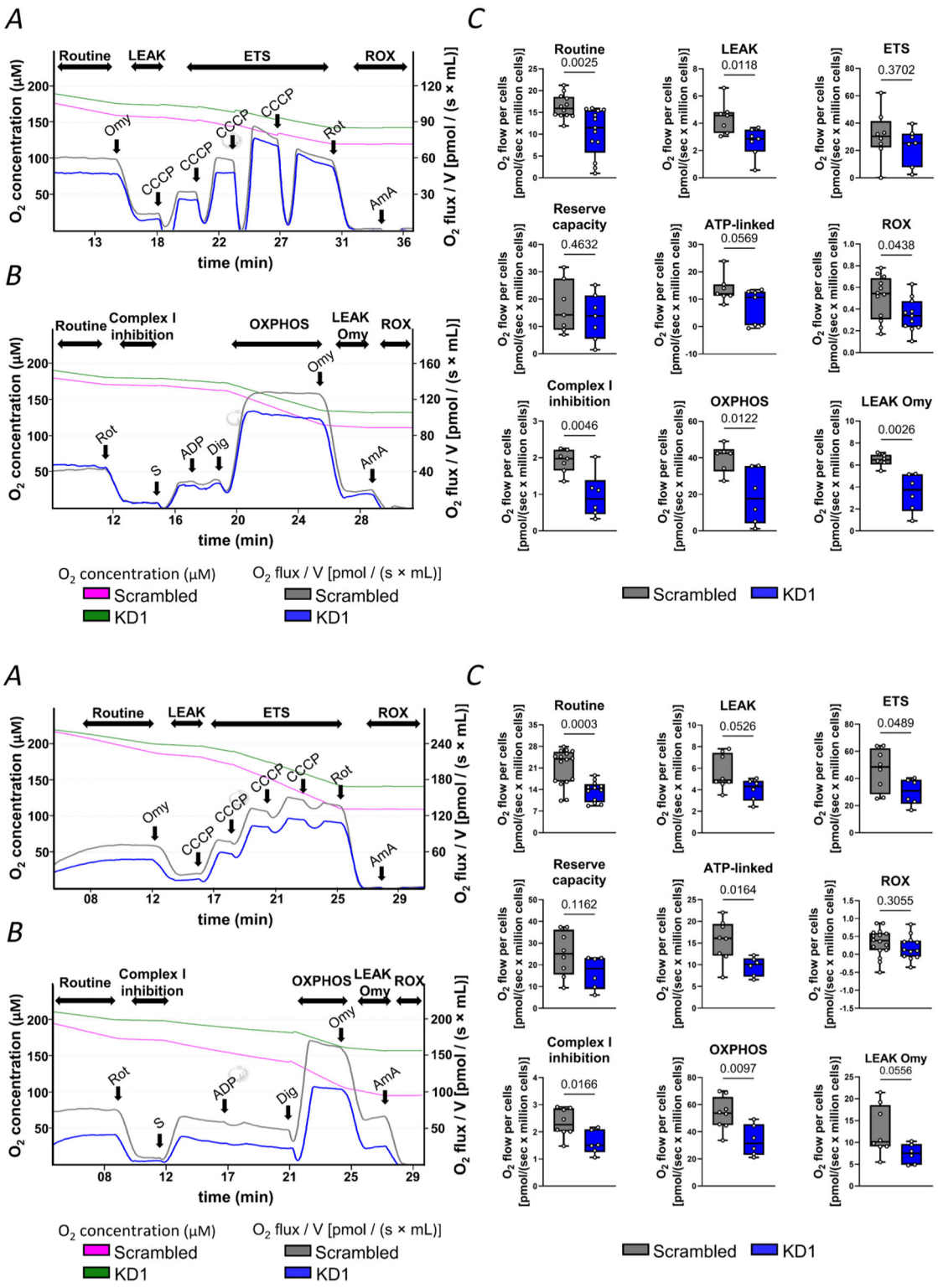


**Figure 9. Functional measurement of mitochondrial respiration**
Representative experimental images show the measurement of mitochondrial respiration with protocol I (*A* and *D*) and protocol II (*B* and *E*). The lines indicate the chamber $O_2$ concentrations (pink and green) and $O_2$ consumption (grey and blue) in the scrambled and Septin7 silenced KD1 myoblasts (*A*, *B* and *C*) ($n$ = 11–13, others: $n$ = 6–8) and myotubes (*D*, *E* and *F*) (Routine and ROX: $n$ = 12–16, others: $n$ = 6–8). *C* and *F*, measured routine respiration, LEAK, ETS, ATP-linked respiration, reserve capacity, ROX, complex I, OXPHOS and LEAK Omy are presented as $O_2$ flux/V [pmol/(s × mL)]. Measurements were normalized to cell number. The box plots demonstrate the median

(horizontal line in the box) and the 25th (lower whisker) and 75th (upper whisker) percentiles. AmA, antimycin A; CCCP, carbonyl cyanide *m*-chlorophenylhydrazone; Dig, digitonin; ETS, electron transport system; Omy, oligomycin; OXPHOS, oxidative phosphorylation; Rot, rotenone; S, succinate.

Skeletal muscle utilizes significant amount of ATP provided mostly by mitochondria. Therefore, it appeared plausible to investigate the role of Septin7 in mitochondria quality control and function in this tissue. C2C12 is the most commonly used model system to investigate skeletal muscle function as a result of rapid differentiation from myoblasts (P) to mature myotubes (D5) expressing skeletal muscle specific proteins and generating force. They contain cytoskeletal network, including septins, as was clearly visible in our cultures. In our previous work, we have already shown that CRISPR/Cas9 technique to completely knock out Septin7 severely affected cell proliferation (Gonczi et al., 2022); therefore, we could only induce partial knockdown by using shRNA. With that, a significant reduction of *septin7* mRNA and protein was achievable in the Septin7 KD cultures. Disrupted Septin7 filaments and cellular structure were indeed clearly detectable in KD myoblast and myotube cultures.

It is plausible to assume that transition from glycolytic myoblasts to metabolically active oxidative phosphorylation-dependent myotubes implies the change in mitochondrial dynamics reflected in the changes of the major regulatory molecules. Indeed, master regulator *PGC1α* mRNA was increased in scrambled myotubes compared to proliferating myoblasts. However, this upregulation could not be detected in KD cells, indicating the importance of Septin7 in mitochondrial dynamics. In the next step, a TaqMan assay revealed a significant decrease in master regulator PGC1α mRNA in *septin7* downregulated myoblasts and myotubes, as well as in those cells where PGC1α level was detected 3 days after the induction of differentiation compared to scrambled cultures. Besides master regulator PGC1α, specific mediators co-ordinate mitochondrial fusion and fission, which are the processes that result in the merging or dividing of mitochondria, respectively. The balance between fusion and fission is inevitable for proper cellular function; however, both processes have special roles. Mitochondrial fission can be triggered by elevated level of cellular stress that can result in mitochondrial dysfunction (Zerihun et al., 2023). Dysfunctional mitochondria eventually have to be removed from the cell, which is initiated by the division of a single mitochondrion into two or more smaller mitochondria, a process called mitochondrial fission. Fission also plays an important role in distributing mitochondria during cell division besides energy metabolism and apoptosis. The major regulator of mitochondrial fission is DRP1 that is recruited from the cytosol to the OMM. Activity of DRP1 is regulated by different post-translational modifications (PTM), such as phosphorylation, SUMOylation, ubiquitination, and *S*-nitrosylation, which alter the oligomerization property of DRP1. PTMs of DRP1 can either activate or inhibit cellular processes. Phosphorylation of DRP1 is a well-known post-translational modification that plays an important role in modulating DRP1 recruitment; consequently, it affects mitochondrial fission. Ser40, Ser44, Ser579, Ser585, Ser592, Ser616, Ser637, Ser656 and Ser693 are the most important and well characterized phosphorylation sites for DRP1. ROCK1, $Ca^{2+}$/calmodulin-dependent protein kinase Iα, AMP kinase and protein kinase D are the best characterized enzymes that can phosphorylate DRP1. Subsequently, dephosphorylation can result in the opposite effect. Phosphorylation of DRP1 at Ser616 promotes mitochondrial fission by facilitating the recruitment of DRP1 to the OMM. Phosphorylation of DRP1 at S616 position can be catalysed by cyclin-dependent kinase 1 (Cdk1–cyclin B), extracellular signal-regulated kinases 1 and 2 (also known as mitogen-activated protein kinase 3 and 1, respectively), protein kinase C δ (PKCδ), Rho-associated protein kinases (ROCK1 and/or ROCK2), $Ca^{2+/}$calmodulin-dependent protein kinase II, Cdk5 and PTEN-induced kinase 1 (PINK1), respectively (Kamerkar et al., 2025). Dual-specificity phosphatase 6 can dephosphorylate DRP1 at S616. On the other hand, phosphorylation of DRP1 at Ser637 by protein kinase A (PKA, also known as cyclic AMP-dependent protein kinase) inhibits the translocation of DRP1 from the cytosol by impairing GTPase activity. Dephosphorylation can be facilitated by protein phosphatase 2A and calcineurin, and phosphoglycerate mutase 5, which could inhibit mitochondrial fission. However, dephosphorylation can also be mediated by calcium-dependent phosphatase calcineurin, which, on the other hand, can promote fission by triggering mitochondrial DRP1 translocation. Taken together, in contrast to S616, the effect of S637 phosphorylation is not consistent, with phosphorylation hampering mitochondrial fission in some cases but activating fission in others.

Mitochondrial dynamics showed stage-dependent changes in scrambled cultures as fission marker *DRP1* (*DNM1L*) was significantly upregulated 3 days after the induction of differentiation indicating that mitochondrial dynamics undergo changes during myogenic differentiation. Septin7 downregulation had an impact on these processes because transcriptome analysis revealed that both the mitophagy (*BNIP3* and *PINK1*) and fission markers (*DNM1L*) were upregulated in KD cells. Although the same mRNA samples were used for

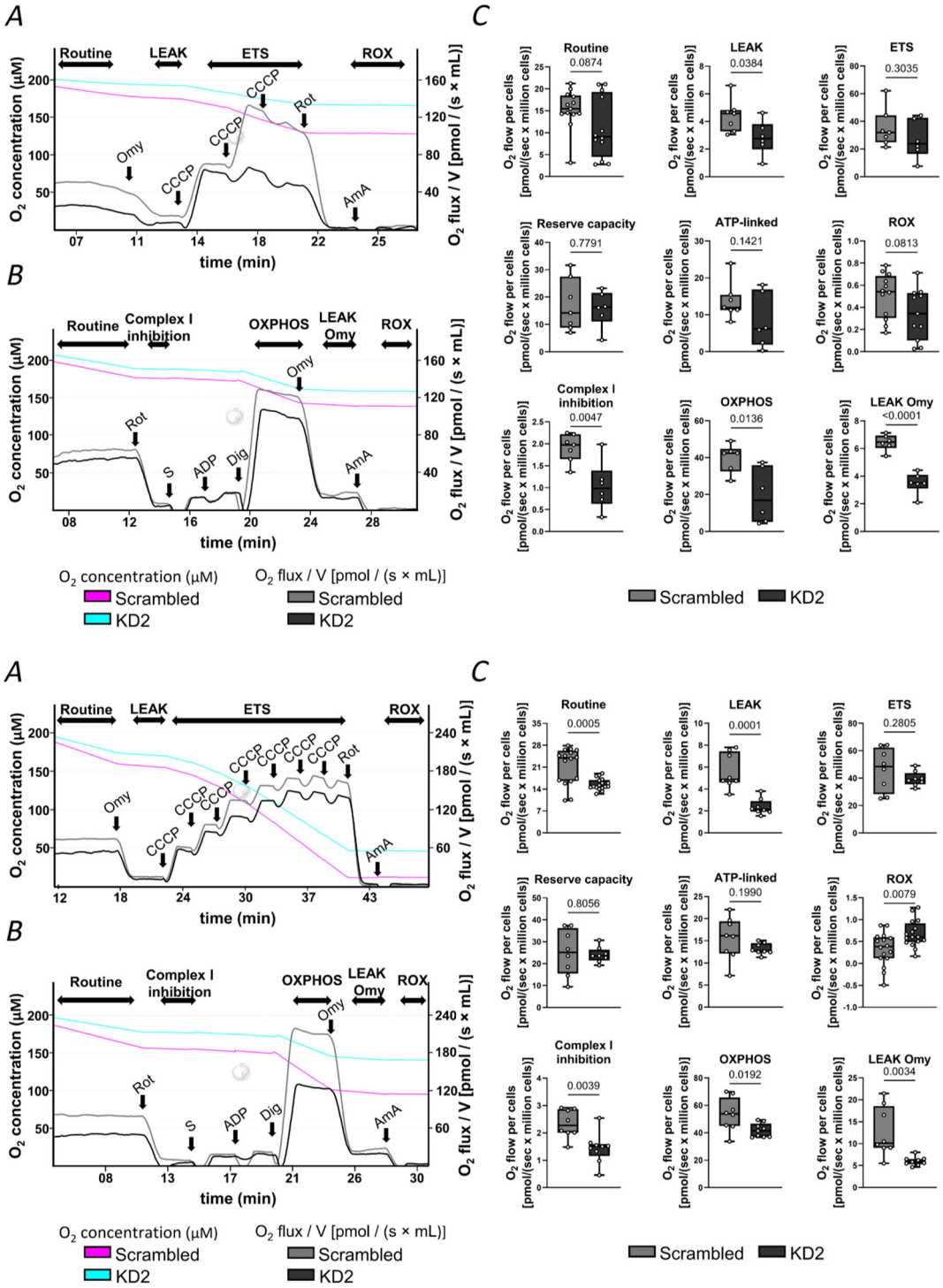


**Figure 10. Functional measurement of mitochondrial respiration on KD2 clone**
Representative experimental images show the measurement of mitochondrial respiration with protocol I (*A* and *D*) and protocol II (*B* and *E*). The lines indicate the chamber $O_2$ concentrations (pink and green) and $O_2$ consumption (grey and blue) in the scrambled and Septin7 silenced myoblasts (*A*, *B* and *C*) (Routine and ROX: $n$ = 11–13, others: $n$ = 6–7) and myotubes (*D*, *E* and *F*) (Routine and ROX: $n$ = 16–17, others: $n$ = 8–9) on KD2 clone. *C* and *F*, measured routine respiration, LEAK, ETS, ATP-linked respiration, reserve capacity, ROX, complex I, OXPHOS and LEAK Omy are presented as $O_2$ flux/V [pmol/(s × mL)]. Measurements were normalized to cell number. The box plots demonstrate the median (horizontal line in the box) and the 25th (lower whisker) and 75th (upper whisker) percentiles (Routine and ROX: $n$ = 11–13, others: $n$ = 5–7). AmA, antimycin A; CCCP, carbonyl cyanide *m*-chlorophenylhydrazone; Dig, digitonin; ETS, electron transport system; Omy, oligomycin; OXPHOS, oxidative phosphorylation; Rot, rotenone; S, succinate.

both RNA-sequencing and TaqMan assays, we obtained different results considering mitochondrial dynamics markers. On the other hand, RNA seq results were confirmed by a TaqMan assay in the case of members of the ETC. Most probably, this is a result of the different sensitivity and methodological approaches of these techniques.

Our experiments also revealed that knockdown of Septin7 alters post-translational modifications of the marker proteins, as confirmed by western blot showing two different post-translational modifications of DRP1. In matured myotubes, the upper band representing one post-translational modification form of DRP1 was significantly downregulated as a result of Septin7 knockdown. On the other hand, the lower band representing a different post-translational modification form of the fission marker was upregulated in Septin7 KD myoblasts. To identify the post-translational modifications, specific antibodies were used to assess different phosphorylation forms of DRP1. We could detect the expression of pDRP1Ser637 in both C2C12 myoblasts and myotubes. Interestingly, we detected the 55 kDa fragment of pDRP1Ser637. Shan et al. (2022) provided evidence about the cleavage of DRP, publication confirming that cleaved DRP1 consists of 25 and 55 kDa fragments. Septin7 downregulation resulted in a significant decrease of pDRP1Ser637 at both stages of differentiation. Because phosphorylation of Ser637 by protein kinase A inhibits the translocation of DRP1 from the cytosol by attenuating GTPase activity, a decreased level of phosphorylation might diminish this procedure. However, recent studies have shown that the phosphorylation status of Ser637 in DRP1 does not determine its recruitment to mitochondria (Yu et al., 2019). Consequently, further experiments are needed to clarify the role of Ser637 phosphorylation in the translocation of DRP1. Regarding Ser616 phosphorylation, we could not detect this form of DRP1 by using specific antibody.

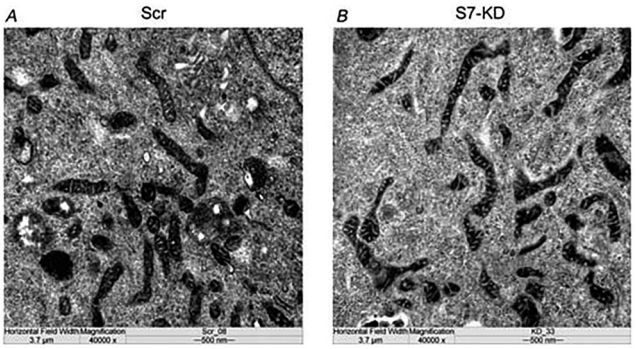


**Figure 11. Septin7 downregulation did not result in a change in the inner mitochondrial structure**
Mitochondrial morphology, distribution and structure of Scr (*A*) and Septin7-KD (*B*) samples analysed by transmission electron microscopy ($n$ = 2 independent cultures; images were taken from seven different slides in the case of scrambled cells and 14 different slides in the case of KD cells, respectively).

Mitochondrial fusion is a complex process where the contents of the merging mitochondria are shared that results in the maintenance of mitochondrial DNA (mtDNA). Fusion is also important in proper cellular energy production besides preventing the possible risks of mitochondrial damage and mutations. Complete fusion requires the merging of both the outer and the inner membrane as well. Outer membrane fusion is facilitated by GTPase proteins Mfn1 and Mfn2 (Jia et al., 2025). Besides co-ordinating mitochondrial fusion, Mfn1 also inhibits cell proliferation, migration and invasion. Mfn2 can form Mfn1/Mfn2 or Mfn2/Mfn2 polymers, promoting perinuclear aggregation and interactions with the endoplasmic reticulum (ER). Naon et al. (2023) described two splice variants of Mfn2: ERMIT2 and ERMIN2. ERMIN2 affects ER morphology, whereas ERMIT2 was localized to the ER mostly at the mitochondria–ER contact sites (MERCS). MERCS play an important role in the regulation of $[Ca^{2+}]_{ic}$, cellular metabolism (Benhammouda et al., 2021), lipid transfer and mitochondrial network dynamics (Chen et al., 2024). In our experiments, mRNA expression of outer mitochondrial membrane fusion marker *Mfn2* was significantly downregulated in Septin7 KD cells compared to scrambled control at the same stage of differentiation. Our results were confirmed in myotubes at the translational level as well. Besides Mfn2, Mfn1 is another GTPase dynamin-related protein located in the outer mitochondrial membrane. The mRNA level of *Mfn1* did not change significantly followed by Septin7 downregulation in C2C12 cells, either at the myoblast or the myotube stage. Interestingly, at the protein level, we could only detect the downregulation of Mfn2 in myotubes followed by Septin7 downregulation.

Complete mitochondrial membrane fusion requires the fusion of the inner mitochondrial membrane as well. Opa1, another GTPase protein, is responsible for the fusion of inner mitochondrial membrane. Recent studies have shown that, besides its importance in fusion, Opa1 also plays a role in *cristae* integrity, respiratory chain supercomplexes assembly and mtDNA maintenance as well. Opa1 also contributes to the regulation of the following processes: mitochondrial $Ca^{2+}$ homeostasis, mitochondrial membrane potential ($\Delta\Psi_m$) and apoptosis (Del Dotto et al., 2017; Del Dotto et al., 2018). Akepati et al. (2008) characterized different Opa1 isoforms in mice. It has been recently revealed that, in humans, alternative splicing of exon 4, 4b and 5b results in eight variants (isoforms) of Opa1 (Del Dotto et al., 2017; Del Dotto et al., 2018). After the precursor protein is transported through the mitochondrial membranes,

the mitochondrial targeting sequence is cleaved by mitochondrial processing peptidase. This cleavage results in the formation of the membrane-anchored Opa1 long forms (l-forms) that can undergo an additional enzymatic modification at the N-terminus producing the short forms (s-forms) that exists as a soluble form in the mitochondrial intermembrane space. Recent models have shown that each isoform can act as a 'pluripotent' isoform because they all have the potential to contribute to the three essential functions: maintenance of mtDNA content, energetics and *cristae* structure. To investigate the exact function of the different forms, selective silencing of the exons was performed in HeLa cells. The experiments showed that exon 4 is important in the maintenance of network and mitochondrial membrane potential, whereas silencing of exon 4b and 5b facilitated apoptosis. On the other hand, depletion of mtDNA was detected in exon 4b-silenced cells and alterated distribution of nucleoids. Based on these experiments, it is plausible to assume that the exon 4 containing variants could be involved in mitochondrial fusion, whereas the exon 5b variants keeps the *cristae* junctions tight aiming to prevent cytochrome *c* mobilization, and the exon 4b variants can play a role in the maintenance of mtDNA. Alternative splicing of Opa1 mRNA is followed by the cleavage of mitochondrial targeting sequence, resulting in the production of long and short forms. The molecular weight of long forms varies within the range 90–120 kDa, whereas, in case of short forms, it is within the range 75–90 kDa, respectively. Short forms support fusion inhibition; subsequent mitochondrial network fragmentation reduces the mitochondrial membrane potential ($\Delta\Psi_m$) that results in the removal of mitochondria by a special form of autophagy called mitophagy. On the other hand, short forms can also help to restore energetic efficiency. Long forms support mitochondrial fusion; long or short forms alone build *cristae*, whereas long and short forms together boost mitochondrial morphology. Maintenance of proper mitochondrial network formation needs a balance of long and short forms comprising at least two isoforms. Thus, multiple Opa1 isoforms are required for mitochondrial dynamics, whereas single isoforms can support certain functions. Consequently, these results confirmed the specific mitochondrial functions of different Opa1 isoforms. Recently, Wang et al. (2021) described the two different models that further explain the possible function of the different isoforms. According to the first model, a mixture of long and short forms is critical for mitochondrial fusion. The second model illustrates that l-Opa1 and s-Opa have different activities; however, l-Opa1 is the only form that promotes fusion. Recent studies by Gilkerson et al. (2021) have shown that Opa1 serves as a link between mitochondrial structure and bioenergetic function. Namely, when the transmembrane potential across the inner membrane ($\Delta\Psi_m$) is intact, long l-Opa1 isoforms promote fusion of the mitochondrial inner membrane. On the other hand, when $\Delta\Psi_m$ is lost, l-Opa1 is cleaved to short, fusion-inactive s-Opa1 isoforms by the stress-sensitive OMA1 metalloprotease, causing the mitochondrial network to collapse to a fragmented population of organelles.

To determine the consequences of Septin7 downregulation on mitochondrial fusion at distinct stages of myogenic differentiation, we investigated Opa1 mRNA and protein expression in scrambled and Septin7 KD myoblasts and myotubes. Mitochondrial inner membrane fusion was affected by Septin7 downregulation in myotubes as indicated by decreased *Opa1* mRNA-expression. On the protein level, several Opa1 isoforms were detected by western blotting. Bands lower than 65 kDa could either be degradation products or specific signals of post-translational modifications, whereas it is difficult to characterize the significance of higher bands. We also analysed the ratio of three Opa1; however, no significant difference could be detected between the expression of the 90, 80 and 65 kDa isoforms.

To assess whether Septin7 plays a role in mitochondrial function, we investigated oxidative phosphorylation in both scrambled and Septin7 KD C2C12cells as well. We first checked the mRNA levels of the most important members of the ETC. Our results indicated that mRNA levels of the members of the ETC (*ATP synthase*, *SDH* and *COX*) were significantly decreased in KD cells; however, in myoblasts and in differentiating cells, this occurred at day 1 after the induction of differentiation.

Mitochondrial function is also affected by miRNAs, the small, non-coding RNA molecules that silence mRNA translation. Recently, some of them were found in mitochondria named mitomiRs that have a crucial role in the regulation of mitochondrial function and metabolism. Resulting from their fundamental role in post-transcriptional regulation of gene expression, microRNAs are powerful regulators of diverse cellular functions including differentiation and function of skeletal muscle, metabolic and redox homeostasis (Saliminejad et al., 2019; Zhang & Liu, 2017). Furthermore, intact regulation of the microRNA expression level is required to maintain mitochondrial health of cells, including their biogenesis, the function of respiratory chain members and widespread metabolic pathways as well (Macgregor-Das & Das, 2018; Storey & Storey, 2020). MitomiRs are microRNAs of nuclear or mitochondrial origin that are localized in mitochondria (Rencelj et al., 2021). *MiR-494-3p* is the most frequently identified mitomiR that regulates both mitochondrial biogenesis and the expression of such important conductor molecules of metabolism as sirtuin enzymes and PGC1$\alpha$ (Geiger & Dalgaard, 2017; Geng et al., 2018); Lemecha et al., 2018). Also, miR-494-3p overexpression resulted in

downregulated mitochondrial proteins in 3T3-L1 beige adipocytes. *miR-494* can affect mitochondrial function as well; namely, it has an inhibitory effect on *PGC1α* gene expression (Lemecha et al., 2018). It has also been shown that endurance training induced increased the expression of PGC1α as a consequence of enhanced oxidative metabolism and altered mitochondrial structure (Bizjak et al., 2021). Decreased Septin7 level resulted in an impaired expression of PGC1α, which might be a reason for diminished oxygen consumption (Suntar et al., 2020). In our experiments, we observed an increasing tendency in *miR-494-3p* expression in KD cultures as C2C12 differentiation progressed.

Alterations in mitochondrial dynamics are also associated with changes of cell metabolism. Metabolic activity is increased in elongated mitochondria, whereas mitochondrial fission can result in decreased mitochondrial ATP generation. However, mitochondrial fission can also be associated with an enhanced degree of oxidative phosphorylation in brown adipocytes and pancreatic β-cells. Besides that, in certain cancer cells, excess amount of fatty acids can also trigger mitochondrial fission, which is important for increased mitochondrial fatty acid oxidation. During myogenic differentiation, energy metabolism changes from glycolytic myoblasts to matured myotubes that rely on oxidative phosphorylation. Because the metabolic switch implies changes in mitochondrial dynamics, its regulation is important for proper myogenic differentiation (Lin et al., 2024). At the beginning of muscle differentiation, mitochondrial fission is activated, whereas fusion is inhibited, resulting in a loose mitochondrial network; however, in later stages, fission is inhibited and fusion is activated, which results in a tight mitochondrial network (Huang et al., 2020). This phenomenon highlights the importance of the adaptive nature of mitochondrial fusion and fission to environmental changes during myogenic differentiation. Studies have shown that Mfn2 is upregulated during myogenic differentiation, which serves as additional evidence for mitochondria undergoing dynamic changes upon request. Lack of Mfn2 results in abnormal mitochondrial respiration with an increased level of ROS, as confirmed by experiments in myoblasts derived from Mfn2-null mice. However, these changes do not inhibit the proliferation and differentiation of myoblasts, which may be the result of a potential compensatory function of Mfn1 that prevents these alterations from affecting muscle development and regeneration (Luo et al., 2021). Fission results in increased number of mitochondria that enhances aerobic respiration and, consequently, ATP production. Subsequently, changes in mitochondria dynamics can lead to an altered activity of the most important enzymes of oxidative phosphorylation. To assess the efficiency of the respiratory chain, key members need to be investigated (Guan et al., 2022). NADH and $FADH_2$ generated by the TCA cycle donate electrons to the ETC at either complex I (NADH:ubiquinone oxidoreductase) or complex II (SDH), respectively. Electrons from complex I and II are shuttled by ubiquinone (in the form of ubiquinol) to complex III ($CoQH_2$-cytochrome *c* reductase), where cytochrome *c* reductase reduces cytochrome *c* followed by the oxidation of this molecule by the complex IV (Timon-Gomez et al., 2018). Finally, the fifth complex terminates ATP synthesis. As expected, changes in dynamic markers resulting from Septin7 downregulation were accompanied by changes in respiratory enzyme levels, based on transcriptome analysis and qPCR experiments. Interestingly, however, this was only true for the myoblast stage. On the other hand, in differentiating myotubes, no difference was detected between S7 KD and Scr cells in the SDH, COX1 and ATP synthase level.

Functional measurements supported the alterations at the mRNA level because the main parameters of both the respiratory electron transfer and oxidative phosphorylation capacity showed significant alterations in both myoblasts and myotubes. Myotubes are metabolically active cells that utilize OXPHOS, which requires large mitochondrial content. On the other hand, myoblasts rely primarily on glycolysis to support their metabolic needs. Consequently, their mitochondria content is much less compared to myotubes (Sin et al., 2016). Interestingly, oxygen consumption was decreased in both myotubes and myoblasts as a result of Septin7 downregulation. In addition, decreased expression of Septin7 resulted in diminished basal respiration, oxidative phosphorylation and oligomycin-inhibited ATP synthesis. Interestingly, activity of the rotenone-sensitive first complex of ETC as well as ROX was only affected in myoblasts. It has been recently shown that ROS can also be produced in other cell compartments, such as cytoplasm, cell membrane, ER and peroxisomes, besides mitochondria. Possible enzyme reactions where ROS can be produced are NADPH oxidases (nicotinamide adenine dinucleotide phosphate, NOX), macrophages, endothelial cells, cytochrome P450-dependent oxygenases, monoaminoxidase; α-glycerophosphate dehydrogenase, electron transfer flavoprotein (ETF) and ETF quinone oxidoreductase (ETF dehydrogenase), respectively (Shu et al., 2023). One of the most important source of cytoplasmic production is the NADPH oxidase (NOXes) family, which is activated upon increased metabolic activity and during the pathogenesis of different diseases. In the ER, protein folding is highly sensitive to changes in redox homeostasis and is one of the main sources of $H_2O_2$ production. In the ER, ER oxidoreductin 1 accepts electrons from peptide substrates via protein disulfide isomerases and transfers them for molecular oxygen generation to produce $H_2O_2$. Peroxisome transfers hydrogen from substrates to $O_2$ to produce $H_2O_2$ through a variety of oxidases under aerobic circumstances. Types

of oxidases can vary between different tissues. The final contribution to $H_2O_2$ production depends on the ratio between the available intracellular oxidant generators (Sies & Jones, 2020). In resting myoblasts, the estimated percentage of NOX-derived cellular $H_2O_2$ production is 40%, whereas ETC accounts for ∼45%, with the remainder coming from other enzymatic sources. Thus, in this case contributions by NOXs and the ETC are commensurate. However, the exact percentage of cellular sources regarding ROS production depends on the cell type as well as the actual metabolic state of the cell, consequently, it can vary upon changing circumstances. Even though NOX4 is located in the inner membrane of the mitochondria, it is not part of the ETC and it only accesses the intermembrane space and cytosol. Therefore, it can be considered as a cytosolic superoxide/hydrogen peroxide producer (Wong et al., 2019).

In the next step, our goal was to check whether functional alterations were reflected in the changes of mitochondrial ultrastructure because studies have shown that changes in mitochondrial network can result in alterations in mitochondrial function (Pernas & Scorrano, 2016; Picard et al., 2013). Glancy et al. (2020) described the functional consequences of different mitochondrial ultrastructure configurations and changes in network structure. The size of the mitochondrial network determines the relative mitochondrial functional capacity within the cell. A large volume of mitochondria means increased mitochondrial functional capacity, wheras a small volume allows space for other cellular structures. In oxidative muscles, an abundant number of mitochondria results in greater mitochondrial functional capacity, whereas a lower volume is available for other cellular components. By contrast, glycolytic muscles with low mitochondrial content have more volume for other cellular compartments resulting in a lower mitochondrial functional capacity. In elongated mitochondria, the relatively large surface area facilitates an interaction with the surrounding environment with respect to the cost of internal functional capacity. In compact mitochondria, on the other hand, the volume is sufficient for internal functional capacity with a reduced surface for interactions with other cellular organisms. Branching mitochondria need long-distance co-ordination to function with a large cost of removal, whereas specialized 3D structures have specific functions. Nanotunnel-shaped mitochondria lack proper space for cristae formation, whereas donut-shaped mitochondria have an increased surface area for interaction with reduced internal volume. Also, individual cristae shape is partially regulated by Opa1. Mitochondria can undergo fission for different reasons. Midzone fission of a healthy mitochondria occurs in the middle region and is part of biogenesis because proliferating cells require a higher number of mitochondria (Kamerkar et al., 2025). On the other hand, peripheral fission is associated with mitophagy when damaged mitochondria are removed from the cell by degradation processes. Mitochondrial damage can occur as a result of the accumulation of different mutations of the mitochondrial genome or as a result of increased oxidative stress (Zerihun et al., 2023). Interestingly, even though we observed functional changes in mitochondrial respiration, transmission electron microscopic analysis did not reveal any morphological difference between scrambled and Septin7 knockdown cells.

In summary, our experiments have revealed that Septin7 plays an important role in regulating the level of molecules that co-ordinate mitochondrial fusion and fission. Diminished level of Septin7 altered the expression of PGC1$\alpha$, DRP1, Opa1 and Mfn2. Besides that, it reduced the colocalization between Septin7 and Opa1, indicating that a decreased level of Septin7 might have functional consequences as well. Indeed, Septin7 downregulation affected mitochondrial respiration as confirmed by the changes of the expression of the key members of oxidative phosphorylation. In conclusion, we have confirmed that cytoskeletal Septin7 significantly alters mitochondrial dynamics and function, indicating a functional link between the cytoskeleton and mitochondria. This might open a novel approach for therapies targeting mitochondria.

## References


Abrisch, R. G., Gumbin, S. C., Wisniewski, B. T., Lackner, L. L., & Voeltz, G. K. (2020). Fission and fusion machineries converge at ER contact sites to regulate mitochondrial morphology. *Journal of Cell Biology*, **219**(4), e201911122.

Addi, C., Bai, J., & Echard, A. (2018). Actin, microtubule, septin and ESCRT filament remodeling during late steps of cytokinesis. *Current Opinion in Cell Biology*, **50**, 27–34.

Akepati, V. R., Muller, E. C., Otto, A., Strauss, H. M., Portwich, M., & Alexander, C. (2008). Characterization of OPA1 isoforms isolated from mouse tissues. *Journal of Neurochemistry*, **106**(1), 372–383.

Akhmetova, K. A., Chesnokov, I. N., & Fedorova, S. A. (2018). [Functional Characterization of Septin Complexes]. *Molekuliarnaia Biologiia*, **52**(2), 137–150.

Banerjee, R., Mukherjee, A., & Nagotu, S. (2022). Mitochondrial dynamics and its impact on human health and diseases: Inside the DRP1 blackbox. *Journal of Molecular Medicine*, **100**(1), 1–21.

Benhammouda, S., Vishwakarma, A., Gatti, P., & Germain, M. (2021). Mitochondria endoplasmic reticulum contact sites (MERCs): Proximity ligation assay as a tool to study organelle interaction. *Frontiers in Cell and Developmental Biology*, **9**, 789959.

Bizjak, D. A., Zugel, M., Treff, G., Winkert, K., Jerg, A., Hudemann, J., Mooren, F. C., Kruger, K., Niess, A., & Steinacker, J. M. (2021). Effects of training status and exercise mode on global gene expression in skeletal muscle. *International Journal of Molecular Sciences*, **22**(22), 12578.

Casanova, A., Wevers, A., Navarro-Ledesma, S., & Pruimboom, L. (2023). Mitochondria: It is all about energy. *Frontiers in Physiology*, **14**, 1114231.

Cavini, I. A., Leonardo, D. A., Rosa, H. V. D., Castro, D., D'Muniz Pereira, H., Valadares, N. F., Araujo, A. P. U., & Garratt, R. C. (2021). The structural biology of septins and their Filaments: An update. *Frontiers in Cell and Developmental Biology*, **9**, 765085.

Chang, C. R., & Blackstone, C. (2010). Dynamic regulation of mitochondrial fission through modification of the dynamin-related protein Drp1. *Annals of the New York Academy of Sciences*, **1201**(1), 34–39.

Chen, S., Sun, Y., Qin, Y., Yang, L., Hao, Z., Xu, Z., Bjorklund, M., Liu, W., & Hong, Z. (2024). Dynamic interaction of REEP5-MFN1/2 enables mitochondrial hitchhiking on tubular ER. *Journal of Cell Biology*, **223**(10), e202304031.

Chen, W., Zhao, H., & Li, Y. (2023). Mitochondrial dynamics in health and disease: Mechanisms and potential targets. *Signal Transduction and Targeted Therapy*, **8**(1), 333.

Cottrill, K. A., Chan, S. Y., & Loscalzo, J. (2014). Hypoxamirs and mitochondrial metabolism. *Antioxid Redox Signaling*, **21**(8), 1189–1201.

Del Dotto, V., Fogazza, M., Carelli, V., Rugolo, M., & Zanna, C. (2018). Eight human OPA1 isoforms, long and short: What are they for? *Biochimica et Biophysica (BBA) – Bioenergetics*, **1859**(4), 263–269.

Del Dotto, V., Mishra, P., Vidoni, S., Fogazza, M., Maresca, A., Caporali, L., McCaffery, J. M., Cappelletti, M., Baruffini, E., Lenaers, G., Chan, D., Rugolo, M., Carelli, V., & Zanna, C. (2017). OPA1 Isoforms in the Hierarchical Organization of mitochondrial functions. *Cell reports*, **19**(12), 2557–2571.

DeWane, G., Salvi, A. M., & DeMali, K. A. (2021). Fueling the cytoskeleton - links between cell metabolism and actin remodeling. *Journal of Cell Science*, **134**(3), jcs248385.

Eiyama, A., & Okamoto, K. (2015). PINK1/Parkin-mediated mitophagy in mammalian cells. *Current Opinion in Cell Biology*, **33**, 95–101.

Gaal, Z., Fodor, J., Olah, A., Radovits, T., Merkely, B., Magyar, J., & Csernoch, L. (2022). Evaluation of muscle-specific and metabolism regulating microRNAs in a chronic swimming rat model. *Journal of Muscle Research and Cell Motility*, **43**(1), 21–33.

Geiger, J., & Dalgaard, L. T. (2017). Interplay of mitochondrial metabolism and microRNAs. *Cellular and Molecular Life Sciences*, **74**(4), 631–646.

Geng, L., Zhang, T., Liu, W., & Chen, Y. (2018). miR-494-3p modulates the progression of in vitro and in vivo Parkinson's disease models by targeting SIRT3. *Neuroscience Letters*, **675**, 23–30.

Gilkerson, R., De La Torre, P., & St Vallier, S. (2021). Mitochondrial OMA1 and OPA1 as gatekeepers of organellar structure/function and cellular stress response. *Frontiers in Cell and Developmental Biology*, **9**, 626117.

Glancy, B., Kim, Y., Katti, P., & Willingham, T. B. (2020). The functional impact of mitochondrial structure across sub-cellular scales. *Frontiers in Physiology*, **11**, 541040.

Gonczi, M., Dienes, B., Dobrosi, N., Fodor, J., Balogh, N., Olah, T., & Csernoch, L. (2021). Septins, a cytoskeletal protein family, with emerging role in striated muscle. *Journal of Muscle Research and Cell Motility*, **42**(2), 251–265.

Gonczi, M., Raduly, Z., Szabo, L., Fodor, J., Telek, A., Dobrosi, N., Balogh, N., Szentesi, P., Kis, G., Antal, M., Trencsenyi, G., Dienes, B., & Csernoch, L. (2022). Septin7 is indispensable for proper skeletal muscle architecture and function. *eLife*, **11**, e75863.

Green, A., Hossain, T., & Eckmann, D. M. (2022). Mitochondrial dynamics involves molecular and mechanical events in motility, fusion and fission. *Frontiers in Cell and Developmental Biology*, **10**, 1010232.

Guan, S., Zhao, L., & Peng, R. (2022). Mitochondrial Respiratory chain supercomplexes: From structure to function. *International Journal of Molecular Sciences*, **23**(22), 13880.

Han, R., Liu, Y., Li, S., Li, X. J., & Yang, W. (2023). PINK1-PRKN mediated mitophagy: Differences between in vitro and in vivo models. *Autophagy*, **19**(5), 1396–1405.

Hirokawa, N., & Takemura, R. (2005). Molecular motors and mechanisms of directional transport in neurons. *Nature Reviews Neuroscience*, **6**(3), 201–214.

Huang, D., Chen, S., Xiong, D., Wang, H., Zhu, L., Wei, Y., Li, Y., & Zou, S. (2023). Mitochondrial dynamics: Working with the cytoskeleton and intracellular organelles to mediate mechanotransduction. *Aging and Disease*, **14**(5), 1511.

Huang, S., Wang, X., Yu, J., Tian, Y., Yang, C., Chen, Y., Chen, H., & Ge, H. (2020). LonP1 regulates mitochondrial network remodeling through the PINK1/Parkin pathway during myoblast differentiation. *American Journal of Physiology-Cell Physiology*, **319**(6), C1020–C1028.

Illescas, M., Penas, A., Arenas, J., Martin, M. A., & Ugalde, C. (2021). Regulation of mitochondrial function by the actin cytoskeleton. *Frontiers in Cell and Developmental Biology*, **9**, 795838.

Jia, G., Song, E., Huang, Q., Chen, M., & Liu, G. (2025). Mitochondrial fusion protein: A new therapeutic target for lung injury diseases. *Frontiers in Physiology*, **16**, 1500247.

Kamerkar, S. C., Liu, A., & Higgs, H. N. (2025). Mitochondrial fission - changing perspectives for future progress. *Journal of Cell Science*, **138**(9), jcs263640.

Kim, J., Mooren, O. L., Onken, M. D., & Cooper, J. A. (2023). Septin and actin contributions to endothelial cell-cell junctions and monolayer integrity. *Cytoskeleton (Hoboken)*, **80**(7–8), 228–241.

Kornmann, B., & Walter, P. (2010). ERMES-mediated ER-mitochondria contacts: Molecular hubs for the regulation of mitochondrial biology. *Journal of Cell Science*, **123**(9), 1389–1393.

Kruppa, A. J., & Buss, F. (2021). Motor proteins at the mitochondria-cytoskeleton interface. *Journal of Cell Science*, **134**(7), jcs226084.

Lemecha, M., Morino, K., Imamura, T., Iwasaki, H., Ohashi, N., Ida, S., Sato, D., Sekine, O., Ugi, S., & Maegawa, H. (2018). MiR-494-3p regulates mitochondrial biogenesis and thermogenesis through PGC1-alpha signalling in beige adipocytes. *Scientific Reports*, **8**(1), 15096.

Lin, F., Sun, L., Zhang, Y., Gao, W., Chen, Z., Liu, Y., Tian, K., Han, X., Liu, R., Li, Y., & Shen, L. (2024). Mitochondrial stress response and myogenic differentiation. *Frontiers in Cell and Developmental Biology*, **12**, 1381417.

Luo, N., Yue, F., Jia, Z., Chen, J., Deng, Q., Zhao, Y., & Kuang, S. (2021). Reduced electron transport chain complex I protein abundance and function in Mfn2-deficient myogenic progenitors lead to oxidative stress and mitochondria swelling. *Federation of American Societies for Experimental Biology Journal*, **35**(4), e21426.

Macgregor-Das, A. M., & Das, S. (2018). A microRNA's journey to the center of the mitochondria. *American Journal of Physiology. Heart and Circulatory Physiology*, **315**(2), H206–H215.

Marquardt, J., Chen, X., & Bi, E. (2019). Architecture, remodeling, and functions of the septin cytoskeleton. *Cytoskeleton (Hoboken)*, **76**(1), 7–14.

Mishra, P., Varuzhanyan, G., Pham, A. H., & Chan, D. C. (2015). Mitochondrial dynamics is a distinguishing feature of skeletal muscle Fiber types and regulates organellar compartmentalization. *Cell Metabolism*, **22**(6), 1033–1044.

Monzel, A. S., Enriquez, J. A., & Picard, M. (2023). Multifaceted mitochondria: Moving mitochondrial science beyond function and dysfunction. *Nature Metabolism*, **5**(4), 546–562.

Naon, D., Hernandez-Alvarez, M. I., Shinjo, S., Wieczor, M., Ivanova, S., Martins de Brito, O., Quintana, A., Hidalgo, J., Palacin, M., Aparicio, P., Castellanos, J., Lores, L., Sebastian, D., Fernandez-Veledo, S., Vendrell, J., Joven, J., Orozco, M., Zorzano, A., & Scorrano, L. (2023). Splice variants of mitofusin 2 shape the endoplasmic reticulum and tether it to mitochondria. *Science*, **380**(6651), eadh9351.

Neubauer, K., & Zieger, B. (2021). Role of septins in endothelial cells and platelets. *Frontiers in Cell and Developmental Biology*, **9**, 768409.

Ney, P. A. (2015). Mitochondrial autophagy: Origins, significance, and role of BNIP3 and NIX. *Biochimica Et Biophysica Acta*, **1853**(10), 2775–2783.

Nolfi-Donegan, D., Braganza, A., & Shiva, S. (2020). Mitochondrial electron transport chain: Oxidative phosphorylation, oxidant production, and methods of measurement. *Redox Biology*, **37**, 101674.

Pagliuso, A., Tham, T. N., Stevens, J. K., Lagache, T., Persson, R., Salles, A., Olivo-Marin, J. C., Oddos, S., Spang, A., Cossart, P., & Stavru, F. (2016). A role for septin 2 in Drp1-mediated mitochondrial fission. *Embo Reports*, **17**(6), 858–873.

Pernas, L., & Scorrano, L. (2016). Mito-morphosis: Mitochondrial fusion, fission, and cristae remodeling as key mediators of cellular function. *Annual Review of Physiology*, **78**(1), 505–531.

Pfanner, N., Warscheid, B., & Wiedemann, N. (2019). Mitochondrial proteins: From biogenesis to functional networks. *Nature Reviews Molecular Cell Biology*, **20**(5), 267–284.

Picard, M., White, K., & Turnbull, D. M. (2013). Mitochondrial morphology, topology, and membrane interactions in skeletal muscle: A quantitative three-dimensional electron microscopy study. *Journal of Applied Physiology*, **114**(2), 161–171.

Popov, L. D. (2020). Mitochondrial biogenesis: An update. *Journal of Cellular and Molecular Medicine*, **24**(9), 4892–4899.

Quinn, P. M. J., Moreira, P. I., Ambrosio, A. F., & Alves, C. H. (2020). PINK1/PARKIN signalling in neurodegeneration and neuroinflammation. *Acta Neuropathologica Communications*, **8**(1), 189.

Rencelj, A., Gvozdenovic, N., & Cemazar, M. (2021). MitomiRs: Their roles in mitochondria and importance in cancer cell metabolism. *Radiology and Oncology*, **55**(4), 379–392.

Saliminejad, K., Khorram Khorshid, H. R., Soleymani Fard, S., & Ghaffari, S. H. (2019). An overview of microRNAs: Biology, functions, therapeutics, and analysis methods. *Journal of Cellular Physiology*, **234**(5), 5451–5465.

Schneider, C. A., Rasband, W. S., & Eliceiri, K. W. (2012). NIH image to ImageJ: 25 years of image analysis. *Nature Methods*, **9**(7), 671–675.

Schwarz, T. L. (2013). Mitochondrial trafficking in neurons. *Cold Spring Harbor Perspectives in Biology*, **5**(6), a011304–a011304.

Shan, S., Liu, Z., Li, L., Zhang, C., Kou, R., & Song, F. (2022). Calpain-mediated cleavage of mitochondrial fusion/fission proteins in acetaminophen-induced mice liver injury. *Human & Experimental Toxicology*, **41**, 9603271221108321.

Shu, P., Liang, H., Zhang, J., Lin, Y., Chen, W., & Zhang, D. (2023). Reactive oxygen species formation and its effect on $CD4^{(+)}$ T cell-mediated inflammation. *Frontiers in Immunology*, **14**, 1199233.

Sies, H., & Jones, D. P. (2020). Reactive oxygen species (ROS) as pleiotropic physiological signalling agents. *Nature Reviews Molecular Cell Biology*, **21**(7), 363–383.

Sin, J., Andres, A. M., Taylor, D. J., Weston, T., Hiraumi, Y., Stotland, A., Kim, B. J., Huang, C., Doran, K. S., & Gottlieb, R. A. (2016). Mitophagy is required for mitochondrial biogenesis and myogenic differentiation of C2C12 myoblasts. *Autophagy*, **12**(2), 369–380.

Storey, K. B., & Storey, J. M. (2020). Mitochondria, metabolic control and microRNA: Advances in understanding amphibian freeze tolerance. *Biofactors*, **46**(2), 220–228.

Suntar, I., Sureda, A., Belwal, T., Sanches Silva, A., Vacca, R. A., Tewari, D., Sobarzo-Sanchez, E., Nabavi, S. F., Shirooie, S., Dehpour, A. R., Xu, S., Yousefi, B., Majidinia, M., Daglia, M., D'Antona, G., & Nabavi, S. M. (2020). Natural products, PGC-1 alpha, and Duchenne muscular dystrophy. *Acta Pharmaceutica Sinica B*, **10**(5), 734–745.

Szabo, L., Telek, A., Fodor, J., Dobrosi, N., Docs, K., Hegyi, Z., Gonczi, M., Csernoch, L., & Dienes, B. (2023). Reduced expression of Septin7 hinders skeletal muscle regeneration. *International Journal of Molecular Sciences*, **24**(17), 13536.

Timon-Gomez, A., Nyvltova, E., Abriata, L. A., Vila, A. J., Hosler, J., & Barrientos, A. (2018). Mitochondrial cytochrome c oxidase biogenesis: Recent developments. *Seminars in Cell & Developmental Biology*, **76**, 163–178.

van Spronsen, M., Mikhaylova, M., Lipka, J., Schlager, M. A., van den Heuvel, D. J., Kuijpers, M., Wulf, P. S., Keijzer, N., Demmers, J., Kapitein, L. C., Jaarsma, D., Gerritsen, H. C., Akhmanova, A., & Hoogenraad, C. C. (2013). TRAK/Milton motor-adaptor proteins steer mitochondrial trafficking to axons and dendrites. *Neuron*, **77**(3), 485–502.

Wang, H., Luo, W., Chen, H., Cai, Z., & Xu, G. (2024). Mitochondrial dynamics and Mitochondrial autophagy: Molecular structure, orchestrating mechanism and related disorders. *Mitochondrion*, **75**, 101847.

Wang, R., Mishra, P., Garbis, S. D., Moradian, A., Sweredoski, M. J., & Chan, D. C. (2021). Identification of new OPA1 cleavage site reveals that short isoforms regulate mitochondrial fusion. *Molecular Biology of the Cell*, **32**(2), 157–168.

Wang, X., Fei, F., Qu, J., Li, C., Li, Y., & Zhang, S. (2018). The role of septin 7 in physiology and pathological disease: A systematic review of current status. *Journal of Cellular and Molecular Medicine*, **22**(7), 3298–3307.

Wong, H. S., Benoit, B., & Brand, M. D. (2019). Mitochondrial and cytosolic sources of hydrogen peroxide in resting C2C12 myoblasts. *Free Radical Biology and Medicine*, **130**, 140–150.

Youle, R. J., & van der Bliek, A. M. (2012). Mitochondrial fission, fusion, and stress. *Science*, **337**(6098), 1062–1065.

Yu, R., Liu, T., Ning, C., Tan, F., Jin, S. B., Lendahl, U., Zhao, J., & Nister, M. (2019). The phosphorylation status of ser-637 in dynamin-related protein 1 (Drp1) does not determine Drp1 recruitment to mitochondria. *Journal of Biological Chemistry*, **294**(46), 17262–17277.

Zerihun, M., Sukumaran, S., & Qvit, N. (2023). The Drp1-mediated mitochondrial fission protein interactome as an emerging core player in mitochondrial dynamics and cardiovascular disease therapy. *International Journal of Molecular Sciences*, **24**(6), 5785.

Zhang, J., & Liu, Y. L. (2017). MicroRNA in skeletal muscle: Its crucial roles in signal proteins, mus cle Fiber type, and muscle protein synthesis. *Current Protein & Peptide Science*, **18**(6), 579–588.

Zhang, J., & Ney, P. A. (2009). Role of BNIP3 and NIX in cell death, autophagy, and mitophagy. *Cell Death and Differentiation*, **16**(7), 939–946.

## Additional information

### Data availability statement

The datasets used and/or analysed during the current study are available from the corresponding author upon reasonable request.

### Competing interests

The authors declare that they have no competing interests.

### Author contributions

JF and AT designed the experiments, interpreted the results, performed data analysis, wrote the original draft of the manuscript, designed and performed mRNA expression analysis, data analyses and interpretation of the results, and revised the manuscript. IGS performed experiments. ZsG performed miRNA experiments and revised the manuscript. MG performed cell culturing and designed the experiments. LSz and BT carried out confocal microscopy experiments and analysis. EG performed experiments. AK-P, ZMK and LJ performed Ouroboros measurements and data analysis. PB revised the manuscript. SzP carried out transcriptome analysis. LC conceived and designed research and revised the manuscript. All authors read and approved the final version of the manuscript submitted for publication. All authors agree to be accountable for all aspects of the work. All persons designated as authors qualify for authorship, and all those who qualify for authorship are listed.

### Funding

This research was supported by National Research, Development and Innovation Office of Hungary grants NKFI OTKA K 137600 (LC) and project No. TKP2021-EGA-18 (under the TKP2021-EGA funding scheme). This project has received funding from the HUN-REN Hungarian Research Network. OTKA K142141. Project no. TKP2021-EGA-19 and TKP2021-EGA-20 have been implemented with the support provided from the National Research, Development and Innovation Fund of Hungary, financed under the TKP2021-EGA funding scheme. SP was supported by the project TKP2021-NKTA-34, which has been implemented with the support provided by the Ministry of Culture and Innovation of Hungary from the National Research, Development and Innovation Fund, financed under the TKP2021-NKTA funding scheme. National Research, Development and Innovation Office of Hungary (NKFI FK 134684). The research was also supported by the Incubation Competence Centre of the Life Sciences Cluster of the Centre of Excellence for Interdisciplinary Research, Development and Innovation of the University of Szeged. AK-P and ZMK are members of the 'New perspectives in skeletal muscle research' group. TKP2021-EGA-28 has been implemented with support provided by the Ministry of Innovation and Technology of Hungary from the National Research, Development and Innovation Fund, financed under the TKP2021-EGA funding scheme.

### Keywords

electron transport, mitochondria, remodelling, septin, skeletal muscle

## Supporting information

Additional supporting information can be found online in the Supporting Information section at the end of the HTML view of the article. Supporting information files available:

**Peer Review History**